PHYSICAL REVIEW A VOLUME 36, NUMBER 10 NOVEMBER 15, 1987

Faddeev-Born-Oppenheimer equations for molecular three-body systems: Application to $H_2{}^+$

A. C. Fonseca and M. T. Peña
Centro Física Nuclear, Avenida Gama Pinto 2, 1699 Lisbon, Portugal

(Received 8 May 1987)

A nonvariational parameter-free molecularlike approach is developed for the three-body problem based on the Faddeev equations. Considering a system of two identical heavy particles (atomic nuclei) and a light one (electron), we study the adiabatic limit of the corresponding Faddeev equation in the absence of interaction between the heavy particles and using general heavy-light potentials that are represented in a separable form through the Hilbert-Schmidt method. The resulting rotationally invariant Faddeev two-center eigenfunctions are used to formulate an ansatz for the solution of the full Hamiltonian where all three particles interact. A set of coupled differential Born-Oppenheimer-like equations is obtained for the movement of the heavy particles. Numerical calculations are shown for the $1s\sigma g$, $2s\sigma g$, $3d\sigma g$, $2p\sigma u$, and $2p\pi u$ electronic states in $H_2{}^+$. The resulting molecular energy curves appear to converge to the exact ones when up to fifteen terms are used in the Hilbert-Schmidt expansion of the Coulomb potential. The noncrossing rule for $2s\sigma g$ and $3d\sigma g$ curves is verified in our work.

I. INTRODUCTION

Since the pioneering work of Faddeev[1] on the formulation of exact three-body theory, later extended by other authors[2] to N-body systems, the solution of the few-body Coulomb problem has been both a challenge and a learning ground. Progress in this field has been slow not only due to the multidimension and multichannel nature of the problem whenever systems of electrons and atomic nuclei are considered, but also due to the difficulty in dealing with the singularities[3] of the Coulomb potential at positive and negative energies. For this reason the initial hope that the new theory would quickly provide more accurate solutions for atomic and molecular systems than the traditional variational or coupled-channel methods used in atomic and molecular physics were replaced by more conservative expectations.[4] In particular, one has learned that sometimes progress is better achieved by using appropriate combinations of old theories with new methods or vice versa. In the present work we attempt to combine the traditional and successful Born-Oppenheimer[5] method for molecular systems with the Faddeev theory for three particles. Although the well-known molecular approach is now part of standard quantum-mechanics text books[6] we find it useful, for later comparison, to review it here in the framework of the three-body problem.

Let us consider a three-body system made up of two identical heavy particles (atomic nuclei) and a light one (electron) interacting by pairwise potentials. The Schrödinger equation in the Jacobian coordinates of Fig. 1(a) reads

$$H\Psi(\mathbf{r},\mathbf{R})=E\Psi(\mathbf{r},\mathbf{R}) , \tag{1}$$

where

$$H=-\frac{\hbar^2}{2\bar{\nu}}\nabla_r^2-\frac{\hbar^2}{2\bar{\mu}}\nabla_R^2+V(R) +v(\,|\,\mathbf{r}+\tfrac{1}{2}\mathbf{R}\,|\,)+v(\,|\,\mathbf{r}-\tfrac{1}{2}\mathbf{R}\,|\,) . \tag{2}$$

While V is the potential between the heavy particles, v is the potential between the light particle and the heavy one. If we denote by m $(\mathcal{M})$ the mass of the light (heavy) particle, $\bar{\mu}$ and $\bar{\nu}$ are the appropriate reduced masses

$$\bar{\nu}=m(2\mathcal{M})/(m+2\mathcal{M}) , \tag{3}$$

$$\bar{\mu}=\frac{\mathcal{M}}{2} . \tag{4}$$

In the standard molecular approximation[6] one considers the eigenfunctions $\psi_i(\mathbf{r},\mathbf{R})$ of the two-center Hamiltonian h,

$$h=-\frac{\hbar^2}{2\bar{\nu}}\nabla_r^2+v(\,|\,\mathbf{r}+\tfrac{1}{2}\mathbf{R}\,|\,)+v(\,|\,\mathbf{r}-\tfrac{1}{2}\mathbf{R}\,|\,) , \tag{5}$$

$$h\psi_i(\mathbf{r},\mathbf{R})=\varepsilon_i(R)\psi_i(\mathbf{r},\mathbf{R}) , \tag{6}$$

as a complete orthogonal basis set to expand Ψ

$$\Psi(\mathbf{r},\mathbf{R})=\sum_j \psi_j(\mathbf{r},\mathbf{R})\Phi_j(\mathbf{R}) . \tag{7}$$

In Eq. (16) $\varepsilon_i(R)$ is the binding energy of the light particle which depends parametrically on the distance R between the two heavy particles. Substituting (7) into (1), multiplying on the left by $\psi_i^*(\mathbf{r},\mathbf{R})$, and integrating in d^3r one obtains a set of coupled differential equations for the Φ_i's,

$$\left[-\frac{\hbar^2}{2\bar{\mu}}\nabla_R^2+V(R)+\varepsilon_i(R)-E\right]\Phi_i(\mathbf{R})=\sum_j\int d^3r\,\psi_i^*(\mathbf{r},\mathbf{R})\left[\frac{\hbar^2}{2\bar{\mu}}[\nabla_R^2\psi_j(\mathbf{r},\mathbf{R})]\Phi_j(\mathbf{R})+\frac{\hbar^2}{2\bar{\mu}}[\nabla_R\psi_j(\mathbf{r},\mathbf{R})]\cdot[\nabla_R\Phi_j(\mathbf{R})]\right]. \tag{8}$$

Formally this is an exact equation where $\varepsilon_i(R)$ acts as an effective potential between the heavy particles due to the multiple exchange of the light one. Nevertheless, in practice, the solution of (6) is not easy to obtain. With the exception of $H_2{}^+$ (Ref. 7) no exact solution of the two-center potential problem exists for a general local interaction v. For any other diatomic molecule, where the number of light particles (electrons) is greater than one, approximation methods based on the linear combination of atomic orbitals (LCAO) (Ref. 8) together with variational parameters are used to obtain the two-center solutions ψ_i in the frame where $\mathbf{R}$ is fixed and the corresponding electronic energy curves are $\varepsilon_i(R)$. If a rotationally invariant Ψ is needed with well-defined total angular momentum J further work is required to generate the wave function in the frame where $\mathbf{R}$ is rotating. This is done using Wigner matrices together with appropriate variational coefficients for each component of the wave function leading to total J.

Although reasonably accurate solutions may be obtained, particularly for low-lying electronic states, one lacks a well-defined prescription on how to improve upon existing results for ψ_i and $\varepsilon_i(R)$ without increasing the number of variational parameters or atomic orbitals. Furthermore, to our knowledge, there is no connection between formally exact N-body theories based on connected kernel equations and the methods used in molecular physics. A first step in that direction is the work of Levin and Krüger[9] where the channel-permuting-array (CPA) theory[10] together with the Born-Oppenheimer approximation is used to study the $H_2{}^+$ molecule. Although the wave function they use is identical to the simplest molecular-orbit (MO) approximation, by using different treatment of the dynamics they get improved results for the equilibrium separation and dissociation energy compared to the standard MO approach based on the asymptotic ($1s$) state. In order to study the convergence properties of the CPA theory[11] they use two different sets of global basis functions: bound hydrogenic states and Hylleraas-Shull-Lowdin states. In either case it was found that there was not even an indication that the results were converging to the exact values when up to 21 terms were included. Both sets yield values for the dissociation energy at the equilibrium separation that are oscillatory and too low. Further work[12] showed that the oscillatory pattern was due to the use of global basis sets and not to CPA formalism. A local-basis-set calculation was undertaken using the finite-element method[13] which showed good convergence results.

In the present work we attempt to formulate a rotationally invariant Born-Oppenheimer-like approach to the molecular three-body problem based on Faddeev's[1] theory. Our aim is to develop a method that may be generalized to more complicated diatomic molecules and gives a clear prescription for how to improve upon existing results in an oscillation-free pattern. Since $H_2{}^+$ is the natural testing ground for any theory that aims to calculate molecular states or energies, we start by treating the simplest molecular three-body problem where a well-understood connected kernel theory such as the Faddeev formalism[1] for three nonrelativistic interacting quantum particles may be used.

Our starting point is the Faddeev equations for the underlying three-body problem in the absence of any heavy-heavy interaction. Since at an intermediate step we want to have access to an exact solution of the two-center problem in the frame where the two heavy particles are rotating in space at distance R from each other, we use the Hilbert-Schmidt expansion[14] (or Weinberg quasiparticle method[15]) to represent the heavy-light potential v in a separable form. As was shown before[16] this reduces the two-center problem given in (6) to the solution of an algebraic equation. With v separable, the above-defined Fadeev equations reduce to a set of coupled one-variable integral equations in the relative momentum $\mathbf{Q}$ between the heavy-light pair and the spectator heavy particle. If we now proceed to take the adiabatic limit $\mathcal{m}/\mathcal{M}\rightarrow 0$ and use closure to write $\bar{\varepsilon}=E-(\hbar^2/2\mu)Q^2$ we find it possible to Fourier transform with respect to the variable $\mathbf{Q}$ leading to a set of coupled homogeneous algebraic equations that depend parametrically on $\mathbf{R}$. In a subsequent transformation we couple the heavy-light orbital angular momentum l with the heavy-heavy orbital angular momentum L to total angular momentum J and parity P to get in each channel J^P discrete solutions $\bar{\varepsilon}_i^{JP}(R)$. The corresponding homogeneous algebraic equation provides, for each R, the necessary weight factors with which each channel component $\psi_i^{JP}(\mathbf{r},\mathbf{R};c)$ enters in the total wave function $\psi_i^{JP}(\mathbf{r},\mathbf{R})$ of well-defined angular momentum J and parity P. Each $\psi_i^{JP}(\mathbf{r},\mathbf{R})$ involves a sum over all components $\sum_c \psi_i^{JP}(\mathbf{r},\mathbf{R};c)$ where c denotes all possible combinations of l, L, and separable component u that couple to J and P. Next we use these two-center wave functions ψ_i^{JP} to write down an ansatz for Ψ^{JP} in the form of a sum over each component $\psi_i^{JP}(r,R;c)$ times an unknown function $\Phi_i^{JP}(R;c)$ of R alone. Proceeding as in the traditional molecular approach one obtains a set of coupled differential equations for the $\Phi_i^{JP}(R,c)$. The main difference between the equations we get and Eq. (8) is that, unlike (8), we always obtain a set of coupled differential equations even when all molecular-orbit states j other than i are neglected. Although we have used a separable representation of v to obtain $\bar{\varepsilon}_i^{JP}(R)$, $\psi_i^{JP}(\mathbf{r},\mathbf{R})$, and a new ansatz for Ψ^{JP}, we take the full potential v in H to generate new molecular-type equations for the $\Phi_i^{JP}(R;c)$. Therefore these are formally exact equations for the molecular three-body problem in a rotationally invariant framework.

In Sec. II we study the adiabatic limit for the two-center Faddeev equations with separable v leading to an exact solution for $\bar{\varepsilon}_i^{JP}(R)$ and in Sec. III we write down the resulting $\psi_i^{JP}(\mathbf{r},\mathbf{R})$. Next we show in Sec. IV how to get the new Faddeev-Born-Oppenheimer equations for the $\Phi_i^{JP}(R;c)$ resulting from the definition of $\Psi^{JP}(\mathbf{r},\mathbf{R})$. Finally, in Sec. V an application to H_2^+ is studied and the results presented for the electronic states $1s\sigma g$, $2s\sigma g$, $3d\sigma g$, $2p\sigma u$, and $2p\pi u$.

II. TWO-CENTER FADDEEV EQUATIONS IN THE STATIC LIMIT

As we mentioned in the Introduction we consider first the Faddeev equations for a system of two identical heavy particles and a light one in the absence of the heavy-heavy interaction. The interaction between the light particle and the heavy particle is v which may be any local short-range or Coulomb-like potential for which a light-heavy t matrix may be defined,

$$t = v + v g_0 t \ , \tag{9}$$

where g_0 is the free resolvent for the underlying two-particle system. For simplicity we assume that v depends only on the spatial coordinates. Let G_0 be the free resolvent for the three-particle system whose momentum-space representation is

$$\langle \mathbf{q}'_k \mathbf{Q}'_k \mid G_0^{-1} \mid \mathbf{q}_k \mathbf{Q}_k \rangle = \left[E - \frac{\hbar^2 q_k^2}{2\nu} - \frac{\hbar^2 Q_k^2}{2\mu} \right] \delta(\mathbf{q}_k - \mathbf{q}'_k)\delta(\mathbf{Q}_k - \mathbf{Q}'_k) \ , \tag{10}$$

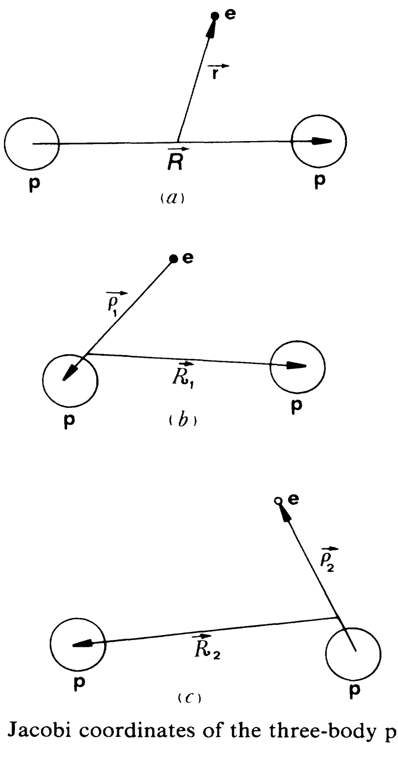

FIG. 1. Jacobi coordinates of the three-body problem.

where, in the usual notation of the three-body problem, $\mathbf{Q}_k$ is the relative momentum between the heavy particle k and the remaining light-heavy pair k. The momentum $\mathbf{q}_k$ is the relative momentum between the particles in pair k. The momenta $\mathbf{q}_k$ and $\mathbf{Q}_k$ are conjugate to the Jacobi variables $\boldsymbol{\rho}_k$ and $\boldsymbol{\mathcal{R}}_k$ shown in Fig. 1(b) and 1(c). the reduced masses ν and μ are

$$\nu = m\mathcal{M}/(m+\mathcal{M}) \ , \tag{11}$$

$$\mu = \mathcal{M}(\mathcal{M}/m)/(m+2\mathcal{M}) \ . \tag{12}$$

Since at this stage we have neglected the heavy-heavy interaction, the resulting Faddeev wave function for the bound-state molecular three-body system[17] involves only two components,

$$\psi = \sum_{k=1}^{2} \bar{\psi}_k \ . \tag{13}$$

The corresponding equation for the wave-function components is

$$\bar{\psi}_k = \sum_{(k' \neq k)} G_0 t_k \bar{\psi}_{k'} \ , \tag{14}$$

where t_k is the light-heavy t matrix for pair k embedded in three-body space. If we now take into account that the two heavy particles are identical, the functional form of the $\bar{\psi}_k$ and t_k is independent of k. Therefore for practical purposes Eq. (14) reduces to a single equation for $\bar{\psi}$ whose momentum-space representation[17] reads

$$\bar{\psi}(\mathbf{q},\mathbf{Q}) = \left[E - \frac{\hbar^2}{2\nu} q^2 - \frac{\hbar^2}{2\mu} Q^2 \right]^{-1} \times \int \frac{d^3 Q'}{(2\pi)^3} \left\langle \mathbf{q} \left| t \left[E - \frac{\hbar^2}{2\mu} Q^2 \right] \right| \mathbf{Q}' + \frac{\mathcal{M}}{m+\mathcal{M}} \mathbf{Q} \right\rangle \times \bar{\psi} \left[\mathbf{Q} + \frac{\mathcal{M}}{m+\mathcal{M}} \mathbf{Q}', \mathbf{Q}' \right] \ , \tag{15}$$

which is a two-vector-variable integral equation. It is well known[18] that Eq. (15) reduces to a single-variable integral equation when a separable representation is used for t. Of all possible choices we use the Hilbert-Schmidt expansion[14] or Weinberg quasiparticle method[15] to obtain t in a separable form. The reason for this choice will become clear in Sec. V. As shown in Appendix A the partial-wave component of v may be written as

$$v_l = \sum_{u}^{N_l} \mid \xi_u^l(\mathcal{E}) \rangle \eta_u^l(\mathcal{E}) \langle \xi_u^l(\mathcal{E}) \mid \ , \tag{16}$$

where u runs over the N_l different separable terms, $\mathcal{E}$ is the light-heavy pair center-of-mass energy, η_u^l the eigenvalues of the $v_l g_0$ kernel at $\mathcal{E}$, and ξ_u^l the corresponding right eigenvector. Substituting (16) in (9) after partial-wave decomposition, we get

$$t_l(\mathcal{E}) = \sum_{u}^{N_l} \mid \xi_u^l(\mathcal{E}) \rangle \tau_u^l(\mathcal{E}) \langle \xi_u^l(\mathcal{E}) \mid \ , \tag{17}$$

where

$$\tau_u^l(\mathcal{E}) = \frac{-\eta_u^l(\mathcal{E})}{1-\eta_u^l(\mathcal{E})} \ . \tag{18}$$

As shown in Appendix A the full momentum-space representation of t reads

$$\langle \mathbf{q}' \,|\, t(\mathcal{E}) \,|\, \mathbf{q} \rangle = \sum_{l,m} \sum_{u}^{N_l} 4\pi Y_{lm}^*(\hat{\mathbf{q}}')\xi_u^l(\mathcal{E};q') \times \tau_u^l(\mathcal{E})\xi_u^l(\mathcal{E};q)Y_{lm}(\hat{\mathbf{q}}) \ . \tag{19}$$

If we now substitute (19) into (15) and define

$$\bar{\psi}(\mathbf{q},\mathbf{Q}) = \sum_{l,m} \sum_{u}^{N_l} \left[E - \frac{\hbar^2}{2\nu}q^2 - \frac{\hbar^2}{2\mu}Q^2 \right]^{-1} \times \xi_u^l \left[E - \frac{\hbar^2}{2\mu}Q^2 ; q \right] Y_{lm}(\hat{\mathbf{q}}) G(\mathbf{Q};ulm) \ , \tag{20}$$

we get a one-variable integral equation for the spectator function G that depends only on the relative momentum between the heavy particle and the remaining light-heavy pair. The resulting equation reads

$$\left[\tau_u^l \left[E - \frac{\hbar^2}{2\mu}Q^2 \right] \right]^{-1} G(\mathbf{Q};ulm) = \sum_{l',m'} \sum_{u'} \int \frac{d^3Q'}{(2\pi)^3} \langle \mathbf{p};ulm \,|\, B(E) \,|\, \mathbf{p}';u'l'm' \rangle \times G(\mathbf{Q}';u'l'm') \ , \tag{21}$$

where

$$\mathbf{p} = \mathbf{Q}' + \frac{\mathcal{M}}{m+\mathcal{M}}\mathbf{Q} \ , \tag{22a}$$

$$\mathbf{p}' = \mathbf{Q} + \frac{\mathcal{M}}{m+\mathcal{M}}\mathbf{Q}' \ . \tag{22b}$$

The driving term B is given by

$$\langle \mathbf{p};ulm \,|\, B(E) \,|\, \mathbf{p}';u'l'm' \rangle = 4\pi \frac{Y_{lm}^*(\hat{\mathbf{p}})\xi_u^l \left[E - \frac{\hbar^2}{2\mu}Q^2 ; p \right] Y_{l'm'}(\hat{\mathbf{p}}')\xi_{u'}^{l'} \left[E - \frac{\hbar^2}{2\mu}Q'^2 ; p' \right]}{E - \frac{\hbar^2}{2\nu}p^2 - \frac{\hbar^2}{2\mu}Q^2} \ . \tag{23}$$

and represents the light-particle exchange diagram shown in Fig. 2. Since the vertex function ξ_u^l depends on the pair energy we must subtract the appropriate relative kinetic energy from the three-body center-of-mass energy E.

If we now take the limit where $m/\mathcal{M} \to 0$ we note that

$$\mathbf{p} = \mathbf{p}' = \mathbf{Q}' + \mathbf{Q} \ , \tag{24}$$

and that

$$\nu = \bar{\nu} = m \ , \tag{25a}$$

$$\mu = \bar{\mu} = \mathcal{M}/2 \ , \tag{25b}$$

$$\mathbf{R} = \mathcal{R}_1 = -\mathcal{R}_2 \ , \tag{25c}$$

$$\mathbf{r} = \boldsymbol{\rho}_1 + \mathbf{R}/2 = \boldsymbol{\rho}_2 - \mathbf{R}/2 \ . \tag{25d}$$

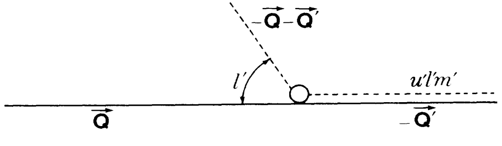

FIG. 2. Driving term for the two-center Faddeev equations.

Since $m \ll \mathcal{M}$ the heavy-particle kinetic energy given by $(\hbar^2/2\mu)Q^2$ and $(\hbar^2/2\mu)Q'^2$ becomes very small compared to the light-particle kinetic energy. In the absence of heavy-heavy interaction we may use closure[19] to define

$$\bar{\varepsilon} \simeq E - \frac{\hbar^2}{2\mu}Q^2 \simeq E - \frac{\hbar^2}{2\mu}Q'^2 \tag{26}$$

as the binding energy of the light particle in the potential field of the two heavy ones. Therefore the driving term B becomes

$$\langle \mathbf{p};ulm \,|\, B(\bar{\varepsilon}) \,|\, \mathbf{p};u'l'm' \rangle = \frac{4\pi Y_{lm}^*(\hat{\mathbf{p}})\xi_u^l(\bar{\varepsilon};p)Y_{l'm'}(\hat{\mathbf{p}})\xi_{u'}^{l'}(\bar{\varepsilon};p)}{\bar{\varepsilon} - \frac{\hbar^2}{2m}p^2} \ , \tag{27}$$

where $\mathbf{p}$ is given by (24). If we also use (26) in the left-hand side of (21) we may easily Fourier transform with respect to the variable $\mathbf{Q}$ after changing the d^3Q' integration into d^3p with the help of (24). The new equation is

$$[\tau_u^l(\bar{\varepsilon})]^{-1} G(\mathbf{R};ulm) = \sum_{l',m'} \sum_{u'} \int \frac{d^3p}{(2\pi)^3} \langle \mathbf{p};ulm \,|\, B(\bar{\varepsilon}) \,|\, \mathbf{p};u'l'm' \rangle \times e^{i\mathbf{p}\cdot\mathbf{R}} G(-\mathbf{R};u'l'm') \ , \tag{28}$$

where the driving term B is given by (27). This is a homogeneous algebraic equation which depends parametrically on $\mathbf{R}$.

The subsequent step involves a partial-wave expansion of the G's together with coupling to total angular momentum J and parity P as is standard procedure in three-body calculations.[17] Defining

$$G^{JP}(R;ulL) = \frac{1}{\hat{J}^2} \sum_{m,MM_j} \int d\Omega_R \, Y^*_{LM}(\hat{\mathbf{R}}) G(\mathbf{R};ulm) C^{l\;L\;J}_{m\,M\,M_j} , \tag{29}$$

and the inverse relation

$$G(\mathbf{R},ulm) = \sum_{J,M_j} \sum_{L,M} G^{JP}(R;ulm) Y_{LM}(\hat{\mathbf{R}}) C^{l\;l\;J}_{m\,M\,M_j} , \tag{30}$$

where $\hat{J} = \sqrt{2J+1}$ and C is a Clebsh-Gordon coefficient, we substitute (29) and (30) in (28), make use of (27), and obtain a set of homogeneous algebraic equations for each J and P that depend parametrically on R alone,

$$[\tau^l_u(\tilde{\varepsilon})]^{-1} G^{JP}(R;ulL) = \sum_{u',l',L'} \langle ulL \,|\, B(\tilde{\varepsilon};R) \,|\, u'l'L' \rangle G^{JP}(R;u'l'L') , \tag{31a}$$

$$\langle ulL \,|\, B(\tilde{\varepsilon},R) \,|\, u'l'L' \rangle = \sum_{\mathcal{L}} \chi^{JP}_{\mathcal{L}}(lL;l'L') \int \frac{p^2 dp}{2\pi^2} \frac{\xi^l_u(\tilde{\varepsilon};p)\xi^{l'}_{u'}(\tilde{\varepsilon},p)}{\tilde{\varepsilon} - \dfrac{\hbar^2}{2m}p^2} j_{\mathcal{L}}(pR) . \tag{31b}$$

The $j_{\mathcal{L}}$ is a spherical Bessel function of order $\mathcal{L}$ and

$$\chi^{JP}_{\mathcal{L}}(lL;l'L') = i^{\mathcal{L}}(-1)^{J+L}(\hat{\mathcal{L}})^2 \hat{l}\hat{l}'\hat{L}\hat{L}' \begin{pmatrix} l' & \mathcal{L} & l \\ 0 & 0 & 0 \end{pmatrix} \begin{pmatrix} L & \mathcal{L} & L' \\ 0 & 0 & 0 \end{pmatrix} \times W(l'lL'L;\mathcal{L}J) , \tag{32}$$

where $\left(\begin{smallmatrix} a & b & c \\ 0 & 0 & 0 \end{smallmatrix}\right)$ is 3-j coefficient and W is a Racah coefficient.

It is worth noting at this stage that Eq. (31) is the two-center equation for the light particle in the frame where the $\mathbf{R}$ is rotating with angular momentum L. The light particle, while interacting with the heavy particle, changes its orbital angular momentum from l to l' while the angular momentum between the heavy particles changes from L to L' such that the total angular momentum J and parity P are conserved. For fixed J, P, and R this homogeneous equation may only have a solution for a discrete set of $\tilde{\varepsilon}^{JP}_i(R)$ where i denotes the different solutions to the problem. Therefore, for each J, P, and i, $\tilde{\varepsilon}^{JP}_i(R)$ is the electronic binding energy as a function of R that emerges from v taken as a sum of separable terms.

III. TWO-CENTER FADDEEV WAVE FUNCTION IN THE STATIC LIMIT

Using (13) and (20) we may now study the Faddeev equation for the two-center wave function in the static limit and write down an expansion for ψ in coordinate space. Starting with Eq. (20) we use (26) together with (25a) to obtain, after Fourier transforming in the variable $\mathbf{Q}$,

$$\bar{\psi}(\mathbf{q},\mathbf{R}) = \sum_u^{N_l} \sum_{l,m} \left[\tilde{\varepsilon} - \frac{\hbar^2}{2m}q^2 \right]^{-1} \xi^l_u(\tilde{\varepsilon};q) \times Y_{lm}(\hat{\mathbf{q}}) G(\mathbf{R};ulm) . \tag{33}$$

Next, using (30) one easily projects out states of well-defined angular momentum J and parity P that correspond to the solution $G^{JP}_i(R;ulL)$ for the eigenvalue $\tilde{\varepsilon}^{JP}_i(R)$,

$$\bar{\psi}^{JP}_i(\mathbf{q},\mathbf{R}) = \sum_{u,l,L} \bar{\psi}^{JP}_i(\mathbf{q},\mathbf{R};ulL) , \tag{34a}$$

$$\bar{\psi}^{JP}_i(\mathbf{q},\mathbf{R};ulL) = \left[\tilde{\varepsilon}^{JP}_i(R) - \frac{\hbar^2}{2m}q^2 \right]^{-1} \xi^l_u(\tilde{\varepsilon}^{JP}_i(R);q) \times \mathcal{Y}^{JM_j}_{lL}(\hat{\mathbf{q}}\hat{\mathbf{R}}) G^{JP}_i(R;ulL) , \tag{34b}$$

where

$$\mathcal{Y}^{JM_j}_{lL} = \sum_{m,M} Y_{lm}(\hat{\mathbf{q}}) Y_{LM}(\hat{\mathbf{R}}) C^{l\;L\;J}_{m\,M\,M_j} . \tag{35}$$

The $\bar{\psi}^{JP}_i(ulL)$ are channel components which we sometimes denote as $\bar{\psi}^{ic}$ where c stands for a possible combination of u, l, and L. As can be seen in (13) the full wave function involves the sum of two components, each one in the appropriate adiabatic Jacobi coordinates

$$\psi^{JP}_i = \frac{1}{\sqrt{2}} [\bar{\psi}^{JP}_i(\boldsymbol{\rho}_1,\mathcal{R}_1) + \bar{\psi}^{JP}_i(\boldsymbol{\rho}_2,\mathcal{R}_2)] , \tag{36}$$

where the $\sqrt{2}$ factor is added to account for the identity of the two heavy particles. The adiabatic coordinates $\mathcal{R}_1$ and $\mathcal{R}_2$ are given by (25c) ($\mathcal{R}_1 = -\mathcal{R}_2 = \mathcal{R}$) and $\boldsymbol{\rho}_1$ and $\boldsymbol{\rho}_2$ are defined as

$$\boldsymbol{\rho}_1 = \boldsymbol{\rho} , \tag{37a}$$

$$\boldsymbol{\rho}_2 = \boldsymbol{\rho} + \mathcal{R} . \tag{37b}$$

The explicit form of ψ reads

$$\psi^{JP}_i(\boldsymbol{\rho},\mathbf{R}) = \frac{1}{\sqrt{2}} \sum_u^{N_l} \sum_{l,L} \int \frac{d^3q}{(2\pi)^3} \left[\tilde{\varepsilon}^{JP}_i(R) - \frac{\hbar^2}{2m}q^2 \right]^{-1} \times \xi^l_u(\tilde{\varepsilon}^{JP}_i(R);q) \times e^{i\mathbf{q}\cdot\boldsymbol{\rho}}[1+(-1)^L e^{i\mathbf{q}\cdot\mathbf{R}}] \times \mathcal{Y}^{JM_j}_{lL}(\hat{\mathbf{q}}\,\hat{\mathbf{R}}) \bar{G}^{JP}_i(R;ulL) , \tag{38}$$

where $\overline{G}$ is related to G through an overall R-dependent normalization constant $\Gamma_i^{JP}(R)$,

$$\overline{G}{}_i^{JP}(R;ulL)=\Gamma_i^{JP}(R)G_i^{JP}(R;ulL)\ , \tag{39}$$

that makes ψ normalized to unity at each R. Comparing (38) with (36) and (34) one can easily identify each component $\overline{\psi}{}_i^{JP}(\boldsymbol{\rho}_1,\mathcal{R}_1)$ and $\overline{\psi}{}_i^{JP}(\boldsymbol{\rho}_2,\mathcal{R}_2)$ which are sometimes denoted as $\overline{\psi}{}_1^{ic}$ and $\overline{\psi}{}_2^{ic}$, respectively.

Thus we have obtained in (38) an exact solution of the two-center problem under the sole approximation of having v represented in a separable form. This is a solution of well-defined angular momentum J and parity P which is an exact nonvariational parameter free eigenfunction of the two-center Hamiltonian h in the $m/\mathcal{M}\rightarrow 0$ limit represented in the basis set that represents v in a separable form. Now we may proceed to obtain the full solution of H by expanding Ψ in the above defined ψ's.

IV. FADDEEV-BORN-OPPENHEIMER EQUATIONS

At this point we are ready to formulate an ansatz for Ψ in terms of the two-center wave functions ψ_i^{JP} previously obtained in such a way that J and P are preserved. In order to simplify the notation we go back to Eq. (38) and write

$$\psi_i^{JP}=\sum_{u,l,L}\psi_i^{JP}(ulL)=\sum_c\frac{1}{\sqrt{2}}(\overline{\psi}{}_1^{ic}+\overline{\psi}{}_2^{ic})\ , \tag{40}$$

where $\psi_i^{JP}(ulL)$ is whatever remains of (38) after the summation in ulL is removed. Denoting each possible combination of u, l, and L as c, we may write down an ansatz for Ψ as

$$\Psi^{JP}(\boldsymbol{\rho},\mathbf{R})=\sum_i\sum_c\psi_i^{JP}(\boldsymbol{\rho},\mathbf{R};c)\Phi_i^{JP}(R;c)\ , \tag{41}$$

where the Φ's are unknown functions of R. Now we go back to the Schrödinger equation (1) and use (41) as a trial function. The Φ's are to be determined from the solution of the resulting differential equation. Before we proceed as in the standard molecular approach a few simplifying assumptions that result from $m \ll \mathcal{M}$ are introduced. As we mentioned before we may use (25) to write the Hamiltonian H in the limit where $m/\mathcal{M}\rightarrow 0$ as

$$H=-\frac{\hbar^2}{2m}\nabla_\rho^2-\frac{\hbar^2}{\mathcal{M}}\nabla_R^2+V(R)+v(\rho)+v(\,|\boldsymbol{\rho}+\mathbf{R}\,|\,)\ . \tag{42}$$

Although this approximation is not really essential to what follows it makes the algebra a great deal easier and the physics more transparent. Therefore we substitute (41) and (1) and use (42) for H. As in the standard approach we multiply on the left by $[\psi_{i'}^{JP}(\boldsymbol{\rho},\mathbf{R};c')]^*$ and integrate in $d^3\rho$ and $d\Omega_R$ to obtain a matrix equation

$$\sum_{i,c}\underline{H}{}_{i'i}^{c'c}(R;JP)\Phi_i^{JP}(R;c)=E\sum_{i,c}\underline{N}{}_{i'i}^{c'c}(R;JP)\Phi_i^{JP}(R;c)\ , \tag{43}$$

where $\underline{N}$ is the norm matrix defined as

$$\underline{N}{}_{i'i}^{c'c}(R;JP)=\int d^3\rho\int d\Omega_R[\psi_{i'}^{JP}(\boldsymbol{\rho},\mathbf{R};c')]^*\psi_i^{JP}(\boldsymbol{\rho},\mathbf{R};c)\ , \tag{44}$$

and $\underline{H}$ a matrix operator that depends not only on R but also on derivatives with respect to R. Because the two-center wave functions ψ_i^{JP} are normalized to unity the norm matrix satisfies the following property:

$$\sum_{c,c'}\underline{N}{}_{i'i}^{c'c}(R;JP)=\delta_{ii'}\ , \tag{45}$$

for all R. Using (38) and (40) to get an explicit form for $\psi_i^{JP}(\boldsymbol{\rho},\mathbf{R};c)$ we obtain

$$\begin{aligned}\underline{N}{}_{i'i}^{c'c}(R;JP)=[\,&A_1^l(R;i'iu'u)\delta_{ll'}\delta_{LL'}+A_2(R;i'ic'c)]\\&\times[\overline{G}{}_{i'}^{JP}(R;c')]^*\overline{G}{}_i^{JP}(R,c)\ ,\end{aligned} \tag{46}$$

where

$$A_1^l(R;i'iu'u)=\int\frac{q^2dq}{2\pi^2}\frac{\xi_{u'}^l(\tilde{\varepsilon}_{i'}(R);q)\xi_u^l(\tilde{\varepsilon}_i(R);q)}{\left[\tilde{\varepsilon}_{i'}(R)-\dfrac{\hbar^2q^2}{2m}\right]\left[\tilde{\varepsilon}_i(R)-\dfrac{\hbar^2q^2}{2m}\right]}\ , \tag{47}$$

$$A_2(R;i'ic'c)=\sum_{\mathcal{L}}\chi_{\mathcal{L}}^{JP}(l'L';lL)\int\frac{q^2dq}{2\pi^2}\frac{\xi_{u'}^{l'}(\tilde{\varepsilon}_{i'}(R);q)\xi_u^l(\tilde{\varepsilon}_i(R);q)}{\left[\tilde{\varepsilon}_{i'}(R)-\dfrac{\hbar^2q^2}{2m}\right]\left[\tilde{\varepsilon}_i(R)-\dfrac{\hbar^2q^2}{2m}\right]}j_{\mathcal{L}}(qR)\ , \tag{48}$$

and $\chi_{\mathcal{L}}^{JP}$ is given by (32). To simplify the notation here we have dropped the JP superscript in $\tilde{\varepsilon}_i(R)$ and will continue to do so. The matrix elements of H may be written as a sum of four terms,

$$\underline{H}=\underline{T}+\underline{L}+\underline{V}+\underline{h}\ , \tag{49}$$

where $\underline{T}$ involves the differential operator with respect to R, $\underline{L}$ is the angular momentum operator in $\hat{\mathbf{R}}$, $\underline{V}$ the heavy-heavy potential, and $\underline{h}$ the two-center Hamiltonian. The matrix elements of $\underline{T}$ are

$$\underline{T}{}_{i'i}^{c'c}(R;JP)=\int d^3\rho\int d\Omega_R[\psi_{i'}^{JP}(\boldsymbol{\rho},\mathbf{R};c)]^*\left[-\frac{\hbar^2}{\mathcal{M}}\left[\frac{d^2}{dR^2}+\frac{2}{R}\frac{d}{dR}\right]\right]\psi_i^{JP}(\boldsymbol{\rho},\mathbf{R};c)\ , \tag{50}$$

where the differential operator acts not only on ψ but also on the Φ to which $\underline{T}$ is applied. In the traditional adiabatic approximation ψ is considered a slowly varying function of R. Thus if one neglects derivatives of ψ with respect to R the matrix elements of $\underline{T}$ become

$$\underline{T}\,{}_{i'i}^{c'c}(R;JP)=\underline{N}\,{}_{i'i}^{c'c}(R;JP)\left[-\frac{\hbar^2}{\mathcal{M}}\left[\frac{d^2}{dR^2}+\frac{2}{R}\frac{d}{dR}\right]\right] . \tag{51}$$

The matrix $\underline{L}$ involves the angular part of the ∇_R^2 operator which is related to $\mathbf{L}^2$. Therefore, starting from

$$\underline{L}\,{}_{i'i}^{c'c}(R;JP)=\int d^3\rho \int d\Omega_R[\psi_{i'}^{JP}(\boldsymbol{\rho},\mathbf{R};c')]^*\left[\frac{\mathbf{L}^2}{\mathcal{M}R^2}\right]\psi_i^{JP}(\boldsymbol{\rho},\mathbf{R};c) , \tag{52}$$

we use the explicit form of $\psi_i^{JP}(\boldsymbol{\rho},\mathbf{R},c)$ to obtain without any further approximation

$$\begin{aligned}\underline{L}\,{}_{i'i}^{c'c}(R;JP)=&\left[\frac{\hbar^2}{\mathcal{M}R^2}\left[\frac{L(L+1)}{2}\right]A_1^l(R;i'iu'u)\delta_{l'l}\delta_{L'L}+\frac{\hbar^2}{\mathcal{M}R^2}\left[\frac{L(L+1)+L'(L'+1)}{2}\right]A_2(R;i'ic'c)\right.\\&\left.+\sum_{K=0}^{\infty}\frac{\hbar^2}{\mathcal{M}R^2}\left[\frac{K(K+1)}{2}\right]A_3^K(R;i'ic'c)\right][\bar{G}\,{}_{i'}^{JP}(R;c')]^*\bar{G}\,{}_i^{JP}(R;c) ,\end{aligned} \tag{53}$$

where A_1 and A_2 are given by (47) and (48), respectively, and

$$A_3^K(R;i'ic'c)=\sum_{\mathcal{L},\mathcal{L}'}\eta_{\mathcal{L}\mathcal{L}'}^{JP}(K;l'L';lL)\int\frac{q^2dq}{2\pi^2}\frac{\xi_{u'}^{l'}(\tilde{\varepsilon}_{i'}(R);q)\xi_u^l(\tilde{\varepsilon}_i(R);q)}{\left[\tilde{\varepsilon}_{i'}(R)-\dfrac{\hbar^2q^2}{2m}\right]\left[\tilde{\varepsilon}_i(R)-\dfrac{\hbar^2q^2}{2m}\right]}j_{\mathcal{L}}(qR)j_{\mathcal{L}'}(qR) . \tag{54}$$

The coefficient $\eta_{\mathcal{L}\mathcal{L}'}^{JP}$ is

$$\begin{aligned}\eta_{\mathcal{L}\mathcal{L}'}^{JP}(K;l'L';lL)=&\,i^{(\mathcal{L}+\mathcal{L}')}(-1)^{\mathcal{L}}\hat{\mathcal{L}}^2\hat{\mathcal{L}}'^2\hat{l}\,\hat{l}'\hat{L}\,\hat{L}'\hat{K}^2\begin{bmatrix}L & \mathcal{L} & K\\ 0 & 0 & 0\end{bmatrix}\begin{bmatrix}L' & \mathcal{L}' & K\\ 0 & 0 & 0\end{bmatrix}\\&\times\sum_{K'}\hat{K}'^2\begin{bmatrix}l & \mathcal{L}' & K'\\ 0 & 0 & 0\end{bmatrix}\begin{bmatrix}l' & \mathcal{L} & K'\\ 0 & 0 & 0\end{bmatrix}\begin{Bmatrix}L & l & J\\ K & \mathcal{L}' & L'\\ \mathcal{L} & K' & l'\end{Bmatrix} .\end{aligned} \tag{55}$$

Although the summation in K runs to infinity in practice it can be truncated since large K implies large $\mathcal{L}$ and $\mathcal{L}'$. Due to the presence of the spherical Bessel functions $j_{\mathcal{L}}$ and $j_{\mathcal{L}'}$ in the integrand of A_3 the contribution of large K values becomes negligible. The third term in (53) is usually called the Coriolis coupling term.

The matrix element of $\underline{V}$ is the simplest one if $V(R)$ is the same for all L. In that case

$$\underline{V}\,{}_{i'i}^{c'c}(R;JP)=\underline{N}\,{}_{i'i}^{c'c}(R;JP)V(R) , \tag{56}$$

where $\underline{N}$ is the norm matrix (44).

Since the matrix elements of $\underline{h}$ involve kinetic energy terms and potential terms we write

$$\underline{h}=\underline{t}+\underline{v} , \tag{57}$$

where $\underline{v}$ involves $v(\rho)$ and $v(|\boldsymbol{\rho}+\mathbf{R}|)$. For $\underline{t}$ we start out with

$$\underline{t}\,{}_{i'i}^{c'c}(R;JP)=\left\langle\psi_{i'}^{JP}(\boldsymbol{\rho};\mathbf{R};c')\left|-\frac{\hbar^2}{2m}\nabla_\rho^2\right|\psi_i^{JP}(\boldsymbol{\rho},\mathbf{R};c)\right\rangle \tag{58}$$

and add and subtract $\tilde{\varepsilon}_{i'}(R)$ to obtain

$$\underline{t}\,{}_{i'i}^{c'c}(R;JP)=\underline{N}\,{}_{i'i}^{c'c}(R;JP)\tilde{\varepsilon}_{i'}(R)+\underline{B}\,{}_{i'i}^{c'c}(R;JP) \tag{59}$$

where

$$\underline{B}\,{}_{i'i}^{c'c}(R;JP)=\left\langle\psi_{i'}^{JP}(\boldsymbol{\rho},\mathbf{R};c')\left[-\tilde{\varepsilon}_{i'}(R)-\frac{\hbar^2}{2m}\nabla_\rho^2\right]\times\psi_i^{JP}(\boldsymbol{\rho},\mathbf{R};c)\right\rangle . \tag{60}$$

Using the appropriate expression for ψ one is led to

$$\underline{B}\,{}_{i'i}^{c'c}(R;JP)=[B_1^l(R;i'iu'u)\delta_{ll'}\delta_{LL'}+B_2(R;i'ic'c)]\times[\bar{G}\,{}_{i'}^{JP}(R;c')]^*\bar{G}\,{}_i^{JP}(R;c) , \tag{61}$$

where

$$B_1^l(R;i'iu'u)=-\int\frac{q^2dq}{2\pi^2}\frac{\xi_{u'}^l(\tilde{\varepsilon}_{i'}(R);q)\xi_u^l(\tilde{\varepsilon}_i(R);q)}{\left[\tilde{\varepsilon}_i(R)-\dfrac{\hbar^2}{2m}q^2\right]} \tag{62}$$

and

$$B_2(R\,;i'ic'c) = \sum_{\mathcal{L}} \chi_{\mathcal{L}}^{JP}(l'L';lL) \times(-1)\int \frac{q^2dq}{2\pi^2}\,\frac{\xi_{u'}^{l'}(\widetilde{\varepsilon}_{i'}(R);q)\,\xi_u^{l}(\widetilde{\varepsilon}_i(R);q)}{\left[\widetilde{\varepsilon}_i(R)-\dfrac{\hbar^2}{2m}q^2\right]} \times j_{\mathcal{L}}(qR)\;. \tag{63}$$

Because of the normalization condition (A8) chosen for ξ, for $i'=i$

$$B_1^l(R\,;iiu'u)=\delta_{u'u} \tag{64}$$

and $B_2=-B$ as given by (31b).

Concerning $\underline{v}$, we first go back to (34), (36), (38), and (40) to note that ψ_i^{JP} is the sum in $c=(ulL)$ of two-channel component $\bar{\psi}_1^{ic}$ in $(\boldsymbol{\rho},\mathbf{R})$ and $\bar{\psi}_2^{ic}$ in $(\boldsymbol{\rho}+\mathbf{R},\mathbf{R})$. If we also denote $v(\rho)$ and $v(\,|\boldsymbol{\rho}+\mathbf{R}|\,)$ as v_1 and v_2, respectively, one may use symmetry arguments to show that

$$\begin{aligned}\underline{v}_{i'i}^{c'c}(R\,;JP)&=\left\langle\frac{1}{\sqrt{2}}(\bar{\psi}_1^{i'c'}+\bar{\psi}_2^{i'c'})\,|\,v_1+v_2\,|\,\frac{1}{\sqrt{2}}(\bar{\psi}_1^{ic}+\bar{\psi}_2^{ic})\right\rangle\\ &=\langle\bar{\psi}_1^{i'c'}\,|\,v_1\,|\,\bar{\psi}_1^{ic}\rangle+\langle\bar{\psi}_1^{i'c'}\,|\,v_1\,|\,\bar{\psi}_2^{ic}\rangle\\ &\quad+\langle\bar{\psi}_2^{i'c'}\,|\,v_1\,|\,\bar{\psi}_1^{ic}\rangle+\langle\bar{\psi}_1^{i'c'}\,|\,v_2\,|\,\bar{\psi}_1^{ic}\rangle\;,\end{aligned} \tag{65}$$

where the $\bar{\psi}$ are given by (34) with $\bar{G}$ instead of G. Since we are using the Hilbert-Schmidt expansion, the channel component $\bar{\psi}_1^{ic}$ is an eigenfunction of g_0v_1 for the eigenvalue $\eta_u^l(\widetilde{\varepsilon}_i)$ (see Appendix A)

$$v_1\bar{\psi}_1^{ic}(\widetilde{\varepsilon}_i)=\eta_u^l(\widetilde{\varepsilon}_i)g_0^{-1}(\widetilde{\varepsilon}_i)\bar{\psi}_1^{ic}(\widetilde{\varepsilon}_i)\;. \tag{66}$$

Therefore

$$\langle\bar{\psi}_1^{i'c'}\,|\,v_1\,|\,\bar{\psi}_1^{ic}\rangle=-\,\eta_{u'}^{l'}(\widetilde{\varepsilon}_{i'}(R))B_1^l(R\,;i'iu'u) \times[\bar{G}_{i'}^{JP}(R\,;c')]^*\bar{G}_i^{JP}(R\,;c)\delta_{l'l}\delta_{L'L}\;, \tag{67}$$

$$\langle\bar{\psi}_1^{i'c'}\,|\,v_1\,|\,\bar{\psi}_2^{ic}\rangle=-\eta_{u'}^{l'}(\widetilde{\varepsilon}_{i'}(R))B_2(R\,;i'ic'c) \times[\bar{G}_{i'}^{JP}(R\,;c')]^*\bar{G}_i^{JP}(R\,;c)\;, \tag{68}$$

$$\langle\bar{\psi}_2^{i'c'}\,|\,v_1\,|\,\bar{\psi}_1^{ic}\rangle=-\eta_u^l(\widetilde{\varepsilon}_i(R))B_2(R\,;ii'c'c) \times[\bar{G}_{i'}^{JP}(R\,;c')]^*\bar{G}_i^{JP}(R\,;c)\;, \tag{69}$$

where B_1 and B_2 are given by (62) and (63), respectively. As for $\langle\psi_1^{i'c'}\,|\,v_2\,|\,\psi_1^{ic}\rangle$ one needs some extra work. Since the calculation is more easily done in configuration space and its difficulty depends on the choice for v, we do it here in a very schematic way. First we make a partial wave expansion for $v(\,|\boldsymbol{\rho}+\mathbf{R}|\,)$,

$$v(\,|\boldsymbol{\rho}+\mathbf{R}|\,)=\sum_{\mathcal{L},\mathcal{M}}v_{\mathcal{L}}(\rho,R)\frac{4\pi}{\hat{\mathcal{L}}^2}Y_{\mathcal{L}\mathcal{M}}(\hat{\rho})Y_{\mathcal{L}\mathcal{M}}^*(-\hat{\mathbf{R}})\;. \tag{70}$$

Next if we denote

$$\bar{\psi}_i^{JP}(\boldsymbol{\rho},\mathbf{R};ulL) =i^l\Theta_u^l(\widetilde{\varepsilon}_i(R);\rho)\mathcal{Y}_{lL}^{JM_j}(\hat{\rho},\hat{\mathbf{R}})\bar{G}_i^{JP}(R\,;ulL)\;, \tag{71}$$

where

$$\Theta_u^l(\widetilde{\varepsilon}_i(R);\rho) =\int\frac{q^2dq}{2\pi^2}\left[\widetilde{\varepsilon}_i(R)-\frac{\hbar^2}{2m}q^2\right]^{-1}\xi_u^l(\widetilde{\varepsilon}_i(R);q)j_l(q\rho)\;, \tag{72}$$

and $\mathcal{Y}$ is given by (35) with $\hat{\rho}$ instead of $\hat{\mathbf{q}}$, we get for the last matrix element

$$\langle\bar{\psi}_1^{i'c'}\,|\,v_2\,|\,\psi_1^{ic}\rangle=\sum_{\mathcal{L}}[\bar{\chi}_{\mathcal{L}}^{JP}(l'L';lL)B_3^{\mathcal{L}}(R\,;i'ic'c)] \times[\bar{G}_{i'}^{JP}(R\,;c')]^*G_i^{JP}(R\,;c)\;, \tag{73}$$

where

$$B_3^{\mathcal{L}}(R\,;i'ic'c)=\int_0^\infty\rho^2d\rho\,\Theta_{u'}^{l'}(\widetilde{\varepsilon}_{i'}(R);\rho)v_{\mathcal{L}}(\rho,R) \times\Theta_u^l(\widetilde{\varepsilon}_i(R);\rho)\;, \tag{74}$$

and

$$\bar{\chi}_{\mathcal{L}}^{JP}(l'L';lL)=i^{l+l'}(-1)^{J+l}\hat{l}'\hat{l}\hat{\mathcal{L}}'\hat{\mathcal{L}} \times\begin{bmatrix}l' & \mathcal{L} & l\\ 0 & 0 & 0\end{bmatrix}\begin{bmatrix}L & \mathcal{L} & L'\\ 0 & 0 & 0\end{bmatrix} \times W(l'lL'L\,;\mathcal{L}J)\;. \tag{75}$$

If an exact solution of the two-center Hamiltonian h is known one can easily check how good are the eigenfunctions ψ_i^{JP} we have developed in Secs. II and III by calculating $\varepsilon_i^{JP}(R)$ as

$$\varepsilon_i^{JP}(R)=\langle\psi_i^{JP}\,|\,h\,\,|\,\psi_i^{JP}\rangle\;, \tag{76}$$

and comparing with the exact solution. Using (59), (61), and (65) together with (45) we get

$$\varepsilon_i^{JP}(R)=\widetilde{\varepsilon}_i^{JP}(R)+\sum_{c,c'}[\underline{B}_{ii}^{c'c}(R\,;JP)+\underline{v}_{ii}^{c'c}(R\,;JP)]\;. \tag{77}$$

Now that we have calculated all matrix elements of the theory and checked the accuracy of our basis set, we can go back to (43) and write down a set of coupled differential equations for the Φ's. To make things as simple as possible we take (51) for $\underline{T}$ which involves neglecting derivatives of ψ with respect to R. Although this is not really needed in our theory it makes the result more transparent. Therefore putting together (51), (53), (56), (59), and (65) with (43) we get

$$\sum_{i,c}\left\{\mathbf{N}_{i'i}^{c'c}(R;JP)\left[-\frac{\hbar^2}{\mathcal{M}}\left(\frac{d^2}{dR^2}+\frac{2}{R}\frac{d}{dR}\right)+V(R)+\tilde{\varepsilon}_{i'}^{JP}(R)-E\right]+[\underline{L}_{i'i}^{c'c}(R;JP)+\underline{B}_{i'i}^{c'c}(R;JP)+\underline{v}_{i'i}^{c'c}(R;JP)]\right\}\Phi_i^{JP}(R;c)=0\;, \tag{78}$$

which replaces the original adiabatic equation (8). There are only two approximations involved in the process of reaching Eq. (78). The first one involves the neglect of terms in $m/\mathcal{M}$ in the original Hamiltonian H defined in (2) to get (42). Considering that $m_e/m_p \simeq 2000$ in molecular physics, terms in $m/\mathcal{M}$ may be calculated in perturbation theory. The second approximation is the neglect of derivatives of ψ with respect to R which is something that can easily be included by working a little harder. Therefore (78) are formally exact equations for the solution of the molecular three-body problem in a rotationally invariant nonvariational parameter-free framework. Now we proceed to test our theory in $H_2{}^+$ molecule where an exact solution exists.

V. APPLICATION TO THE $H_2{}^+$ MOLECULE

With the theory developed in Secs. II–IV we now solve the corresponding equations for the $H_2{}^+$ molecule where an exact solution of the two-center problem is already known.[7] First we solve (31a) and (31b) to obtain $\tilde{\varepsilon}_i^{JP}(R)$ and $G_i^{JP}(R;ulL)$. The $\xi_u^l(\tilde{\varepsilon};p)$ are given in Appendix C. They are the eigenfunctions of the $v_l g_0(\tilde{\varepsilon})$ kernel at the energy $\tilde{\varepsilon}$ where v is the potential between the electron and the proton. The corresponding eigenvalue $\eta_u^l(\tilde{\varepsilon})$ is given by

$$[\eta_u^l(\tilde{\varepsilon})]^{-1}=\frac{n}{z}\delta\;, \tag{79}$$

where

$$n=u+l\;, \tag{80}$$

$$\delta=\sqrt{-\tilde{\varepsilon}}\;, \tag{81}$$

in units of $\hbar=2m=1$. If we also take the rydberg as the unit of energy, the corresponding unit of length is the Bohr radius. In those units

$$v(r)=-2Z/r\;, \tag{82}$$

where Z is the charge number of the atomic nucleus which is $Z=1$ for hydrogen. As mentioned before the index u runs from 1 to N_l where N_l is the number of separable terms that are taken at each l, and n is the principal quantum number.

In the framework of the equations we propose in Sec. II, the simplest approach involves a single-term separable representation of v through the lowest eigenvector $\xi_1^0(\tilde{\varepsilon};p)$ which corresponds to the first hydrogenic state $n=1$, $l=0$. From (32) we find that for $l=l'=0$ we get only $\mathcal{L}=0$ which implies $L=L'$. Therefore

$$\chi_{\mathcal{L}}^{JP}(0L;0L')=\delta_{\mathcal{L}0}\delta_{LL'}\delta_{JL}(-1)^J\;. \tag{83}$$

Using (31a), (31b), (18), (79), and (83) we get a single equation for $G(R)=G^{JP}(R;10J)$,

$$\left[1-\frac{1}{Z}\sqrt{-\tilde{\varepsilon}}\right]G(R)=(-1)^J\int\frac{p^2dp}{2\pi^2}\frac{[\xi_1^0(\tilde{\varepsilon};p)]^2}{\tilde{\varepsilon}-p^2}j_0(pR)G(R)\;. \tag{84}$$

At $R=0$ we may use the normalization condition for the ξ's shown in (A8) to obtain

$$\left[1+(-1)^J-\frac{1}{Z}\sqrt{-\tilde{\varepsilon}}\right]G(0)=0\;. \tag{85}$$

For J even a nontrivial solution to (85) implies

$$\tilde{\varepsilon}_1^{J+}(0)=-(2Z)^2\;, \tag{86}$$

which for $Z=1$ gives $\tilde{\varepsilon}_1^{J+}(0)=-4$ Ry. At $R=\infty$ the right-hand side of (84) goes to zero and we get $\tilde{\varepsilon}_1^{J+}(\infty)=-Z^2$ which for $Z=1$ becomes $\tilde{\varepsilon}_1^{J+}(\infty)=-1$ Ry. In the united-atom limit ($R=0$) one has two protons interacting with a single electron which leads to a hydrogenlike system with $Z=2$. Using (B13) with $n=1$ the ground-state energy of such system becomes $\varepsilon_1=-4$ Ry. In the separated-atom limit ($R=\infty$) the electron goes with either one of the protons leading to $\varepsilon_1=-1$ Ry. Therefore our effective potential $\tilde{\varepsilon}_1^{J+}(R)$ resulting from the solution of the Faddeev two-center equation (84) with a single-term separable representation of the potential $v=-2Z/r$ is exact at both extremes. This result is not independent of the method chosen to obtain a separable representation for v. It is there that lies the great advantage of the Hilbert-Schmidt (HS) representation. Had we taken the Ernst, Shakin, and Thaler (EST) method,[20] the unitary pole expansion[21] (UPE), or the Adhikari-Sloan[22] (AS) approach the resulting one-term approximation for the calculation of $\tilde{\varepsilon}_1^{J+}(0)$ would differ from the exact result. If EST (or UPE at the ground-state pole) is used instead of HS, one gets $\tilde{\varepsilon}_1^{J+}(0)=-3.343\,15$ Ry for a single term in the expansion of the e-p Coulomb potential which does not converge to -4 Ry when more terms are used in the expansion. Nevertheless, like HS, EST is exact in the separated-atom limit ($R=\infty$) since one may explicitly introduce there as many bound-state poles of the e-p potential as one needs; the existence of each pole is associated with a single term in the expansion. This is not the case for UPE or for any version of AS that does not coincide with HS or EST.

For intermediate R we have to solve (84). Using (C8) for ξ_1^0, the integral involving $j_0(kR)$ may be easily done analytically. A nonzero $G(R)$ implies the solution of a transcendental equation which for L even reads

$$1-\frac{1}{Z}\delta+(1+\delta R)e^{-\delta R}=0\;, \tag{87}$$

$$\delta=\sqrt{-\tilde{\varepsilon}}\;. \tag{88}$$

The corresponding $\tilde{\varepsilon}_1^{j+}(R)$ is shown in Table I and the normalized wave function $\psi(\boldsymbol{\rho},\mathbf{R})$ resulting from (38) reads

$$\psi_1^{J+}(\boldsymbol{\rho},\mathbf{R})=[4\pi\sqrt{2(1+S)}]^{-1} \times[R_{10}(\rho)+R_{10}(|\boldsymbol{\rho}+\mathbf{R}|)]_{\alpha_1=\delta(R)}\,, \tag{89}$$

where R_{10} is the radial part of the hydrogen wave function given in (B1) with α_1 changed into $\delta(R)$ at each R, and

$$S=(1+\delta R+\tfrac{1}{3}\delta^2 R)e^{-\delta R}\,, \tag{90}$$

$$\delta\equiv\delta(R)=\sqrt{-\tilde{\varepsilon}_1^{J+}(R)}\,. \tag{91}$$

Therefore in lowest-order approximation we get a two-center wave function similar to the well-known LCAO wave function. At $R=0$ it becomes an exact solution of the corresponding united-atom problem, and at $R=\infty$ it coincides with LCAO which is also an exact solution in the separated-atom limit.

In order to check the accuracy of the wave function (89) against an exact solution of h for the lowest molecular-orbital state ($1s\sigma g$ in the united-atom notation) we calculate (76)

$$\varepsilon_1^{J+}(R)=\langle\psi_1^{J+}\,|\,h\,|\,\psi_1^{J+}\rangle\,. \tag{92}$$

Since all integrals involving $\underline{B}(R)$ and $\underline{v}(R)$ (see Sec. IV) may be done analytically we get

$$\varepsilon_1^{J+}(R)=\tilde{\varepsilon}_1^{J+}(R)+\frac{1}{1+S}\{2\delta^2[1+(1+\delta R)e^{-\delta R}] -2\delta[1+2(1+\delta R)e^{-\delta R}] -\frac{2}{R}[1-(1+\delta R)e^{-2\delta R}]\}\,. \tag{93}$$

The resulting $\varepsilon_1^{J+}(R)$ is also shown in Table I and is compared with the exact $1s\sigma g$ result. Since $\tilde{\varepsilon}_1^{J+}(R)$ is exact at $R=0$ the second term in (93) is zero in that limit where $\delta=2$. If we make $\tilde{\varepsilon}_1^{J+}(R)=\varepsilon_1=-1$ for all R, then $\delta=\alpha_1=1$ and (89) becomes the standard LCAO wave function. Consequently (93) turns into the LCAO two-center energy

$$\varepsilon_{\text{LCAO}}(R)=-1-\frac{2}{1+S}\left[(1+R)e^{-R}+\frac{1}{R}[1-(1+R)e^{-2R}]\right], \tag{94}$$

which is also shown in Table I for comparison. If one adds to the two-center energy $\varepsilon(R)$ the proton-proton Coulomb repulsion and subtracts the asymptotic energy $\varepsilon(\infty)$, one gets the potential energy curve for the $1s\sigma g$ state which is responsible for a bound $H_2{}^+$ molecule. Defining

$$E_1^{J+}(R)=\varepsilon_1^{J+}(R)+\frac{2}{R}-\varepsilon_1^{J+}(\infty)\,, \tag{95}$$

we show in Fig. 3 our lowest-order result compared to the known exact solution. The electronic Bohr radius is $a_0=0.528\,177$ Å.

In order to improve on the one-term approximation in a consistent way we include more terms in the separable expansion of v. This also leads to the possibility of finding other molecular-orbital states which correspond

TABLE I. Two-center binding energies (rydbergs) for a single ($1s$)-state representation of the Coulomb potential.

R/a_0	$-\tilde{\varepsilon}_1^{J+}(R)$	$-\varepsilon_1^{J+}(R)$	$1s\sigma g$ exact	LCAO ($1s$)
0.0	4.000 00	4.000 00	4.000 00	3.000 00
0.2	3.769 84	3.856 77	3.857 41	2.984 74
0.4	3.358 98	3.597 97	3.601 57	2.944 93
0.6	2.970 24	3.333 90	3.343 01	2.882 92
0.8	2.645 88	3.093 63	3.108 95	2.802 99
1.0	2.382 74	2.882 50	2.903 56	2.710 76
1.2	2.169 38	2.698 90	2.724 61	2.611 55
1.4	1.995 00	2.539 37	2.568 53	2.509 66
1.6	1.851 07	2.400 39	2.431 86	2.408 33
1.8	1.731 07	2.278 79	2.311 62	2.309 88
2.0	1.630 13	2.171 91	2.205 25	2.215 88
2.2	1.544 54	2.077 53	2.110 76	2.127 29
2.4	1.471 48	1.993 85	2.026 42	2.044 65
2.6	1.408 75	1.919 36	1.950 90	1.968 19
2.8	1.354 65	1.852 82	1.882 99	1.897 88
3.0	1.307 81	1.793 20	1.821 78	1.833 57
3.2	1.267 14	1.739 63	1.766 47	1.774 96
3.4	1.231 74	1.691 38	1.716 39	1.721 73
3.6	1.200 89	1.647 83	1.670 97	1.673 48
3.8	1.173 98	1.608 44	1.629 71	1.629 82
4.0	1.150 49	1.572 76	1.592 16	1.590 36
5.0	1.071 24	1.437 50	1.448 84	1.443 21
6.0	1.032 30	1.351 26	1.357 26	1.352 79
7.0	1.014 01	1.293 84	1.296 90	1.294 20
8.0	1.005 96	1.253 58	1.255 14	1.253 66
9.0	1.002 47	1.223 79	1.224 61	1.223 81

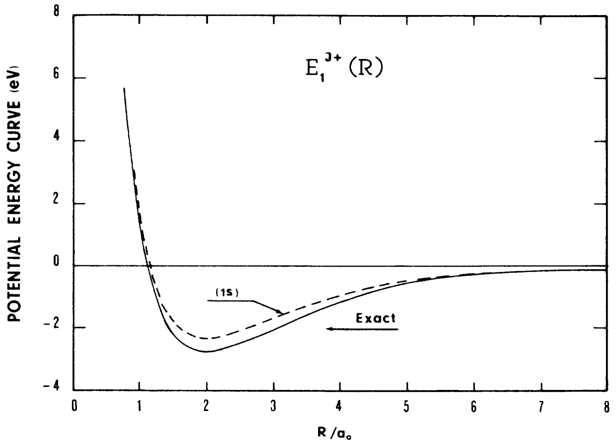

FIG. 3. Potential energy curve (eV) vs R (Bohr radii). The solid line denotes the exact $1s\sigma g$ potential (Ref. 7) while the dashed line is the result of our calculation with a one-term expansion for v.

TABLE II. Possible channels of the two-center Faddeev equation (31) for $J=0^+$ and $J=2^+$.

		$J^P=0^+$	
c	u	l	L
1	1	0	0
2	2	0	0
3	1	1	1
		$J^P=2^+$	
c	u	l	L
1	1	0	2
2	2	0	2
3	1	1	1
4	1	1	3

to excited electronic configurations that bear support on states with $n>1$ either on the united-atom limit or the separated-atom extreme. Since we work with states of well-defined angular momentum J and parity P, we note that the lowest state only emerges for J even and parity $+$. Furthermore we find that $\tilde{\varepsilon}_i^{JP}(R)$ is the same for all J's of a given parity. Nevertheless the resulting wave function ψ_i^{JP} depends on J not only through the number of channels $c\equiv(ulL)$ that couple to J^P but also through the coefficients $\bar{G}_i^{JP}(R;c)$ that result from the solution of (31a). In Table II we present the channels involved in the solution of (31) for $J^P=0^+$ and 2^+ for a calculation involving the three lowest hydrogenic states up to $n=2$. Therefore we study first the lowest positive parity solution of (31) $\tilde{\varepsilon}_1^{J+}(R)$ corresponding to $1s\sigma g$ as the number of terms in the separable expansion of v is increased from one to 15. Denoting $n_{\max}$ and $l_{\max}$ the largest n

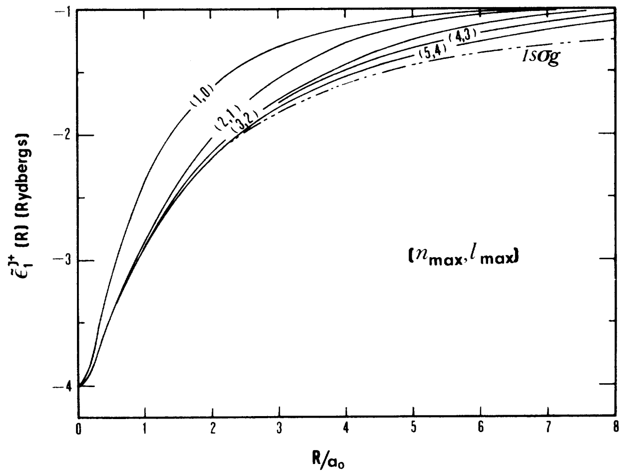

FIG. 4. Two-center binding energy $\tilde{\varepsilon}_1^{J+}(R)$ (rydbergs) vs R (Bohr radii) for increasing number of separable terms in Eq. (31). The dash–double-dotted line is the exact $1s\sigma g$ result (Ref. 7).

TABLE III. Calculated electronic binding energy $-\varepsilon_1^{J+}(R)$ (rydbergs) versus R (Bohr radii) for increasing number of terms used in the separable representation of v. The exact $1s\sigma g$ result is shown for comparison.

			$(n_{\max},l_{\max})$			
R/a_0	(1,0)	(2,1)	(3,2)	(4,3)	(5,4)	$1s\sigma g$ exact
0.0	4.000 00	4.000 00	4.000 00	4.000 00	4.000 00	4.000 00
0.2	3.856 76	3.856 13	3.856 92	3.857 16	3.857 25	3.857 31
0.4	3.597 96	3.596 23	3.600 27	3.601 15	3.601 46	3.601 57
0.6	3.333 90	3.334 08	3.340 81	3.342 31	3.342 90	3.343 01
0.8	3.093 63	3.097 13	3.105 80	3.108 09	3.108 87	3.108 95
1.0	2.882 50	2.888 53	2.899 47	2.902 52	2.903 36	2.903 56
1.2	2.698 90	2.705 95	2.719 66	2.723 25	2.724 14	2.724 61
1.4	2.539 37	2.546 15	2.562 70	2.566 65	2.567 73	2.568 53
1.6	2.400 39	2.406 05	2.425 00	2.429 26	2.430 75	2.431 86
1.8	2.278 79	2.282 89	2.303 42	2.308 14	2.310 22	2.311 62
2.0	2.171 91	2.174 31	2.195 38	2.200 87	2.203 63	2.205 25
2.2	2.077 53	2.078 28	2.098 81	2.105 46	2.108 89	2.110 76
2.4	1.993 85	1.993 09	2.012 02	2.020 26	2.024 27	2.026 42
2.6	1.919 36	1.917 32	1.933 68	1.943 89	1.948 35	1.950 90
2.8	1.852 82	1.849 76	1.862 72	1.875 19	1.879 97	1.882 99
3.0	1.793 19	1.789 40	1.798 29	1.813 15	1.818 15	1.821 78
3.2	1.739 63	1.735 40	1.739 68	1.756 94	1.762 12	1.766 47
3.4	1.691 38	1.687 01	1.686 34	1.705 82	1.711 23	1.716 39
3.6	1.647 82	1.643 61	1.637 78	1.659 19	1.664 93	1.670 97
3.8	1.608 44	1.604 63	1.593 61	1.616 53	1.622 75	1.629 71
4.0	1.572 75	1.569 59	1.553 51	1.577 40	1.584 29	1.592 16
5.0	1.437 49	1.438 91	1.405 07	1.424 17	1.436 48	1.448 84
6.0	1.351 26	1.354 48	1.324 42	1.325 01	1.340 88	1.357 26
7.0	1.293 84	1.295 92	1.282 49	1.266 31	1.277 93	1.296 90
8.0	1.253 58	1.254 50	1.251 46	1.235 01	1.237 04	1.255 14
9.0	1.223 79	1.224 14	1.223 84	1.215 64	1.210 97	1.224 61

and l included, we show in Fig. 4 how $\tilde{\varepsilon}_1^{J+}(R)$ changes when $(n_{\max},l_{\max})$ takes the values running from (2,1) to (5,4). Likewise, in Table III we show the values obtained for $\varepsilon_1^{J+}(R)$ resulting from the calculation of (76) for increasing number of terms. Compared with the exact $1s\sigma g$ curve we find that the calculated $\varepsilon_1^{J+}(R)$ appears to converge monotonically to the exact result. At all R we find that from an initial value for ε with $n_{\max}=1$ and $l_{\max}=0$, one develops first a larger discrepancy relative to the exact results before monotonic convergence is reached for increasing $(n_{\max},l_{\max})$. As shown in Table III, for $R=4a_0$, one gets -1.57275 Ry with a single term in the expansion of v which moves to -1.55351 Ry when all terms up to (3,2) are used for v. This initial departure from the exact answer is reversed when higher hydrogenic states are included. The results becomes -1.58429 Ry when $n_{\max}=5$ and $l_{\max}=4$. For a given R the weight factors $\bar{G}_1^{J+}(R,c)$ change as more separable terms are included. This is shown in Table IV for $R=4a_0$ and $(n_{\max},l_{\max})$ running from (1,0) to (5,4). The weight factor of the $(1s)$ term decreases first when the number of terms increases from (1,0) to (3,2). At (4,3) the trend is reversed and as shown in Table III from then on $\varepsilon_1^{J+}(4a_0)$ converges monotonically. Therefore one may conclude that at a given R, once the dominant hydrogenic states are included, $\varepsilon_1^{J+}(R)$ converges monotonically to the exact electronic molecular energy. For 15 terms in the expansion of v we get three-digit accuracy for R between zero and almost four Bohr radii. In Fig. 5 we compare the calculated $E_1^{J+}(R)$ with $n_{\max}=5$ and $l_{\max}=4$ to the exact $1s\sigma g$ potential energy curve. At $R=2a_0$ which nearly corresponds to the position of the minimum $E_1^{J+}=-2.7616$ eV and $E_{1s\sigma g}=-2.7911$ eV. Since in Table III at $R=8a_0$ one finds that for $(n_{\max},l_{\max})=(5,4)$ the trend away from the exact $1s\sigma g$ result has just been reversed, we expect that by $(n_{\max},l_{\max})=(8,7)$ we should be able to reproduce the exact $1s\sigma g$ potential energy curve in the whole range of R values between zero and $8a_0$. Due to computer limitations at this time we restricted ourselves to just 15 terms in the expansion of v which corresponds to $(n_{\max},l_{\max})=(5,4)$. Finally, in Fig. 6 we show $\bar{G}_1^{0+}(R,c)$ with $l=L$ as a function of R for different channels and $(n_{\max},l_{\max})=(5,4)$. Although, as expected, the dominant component corresponds to the $(1s)$ state, we find that $(2s)$, $(3s)$, $(2p)$, $(3p)$, and $(3d)$ states have comparable strength that increases with R before vanishing at $R\rightarrow\infty$.

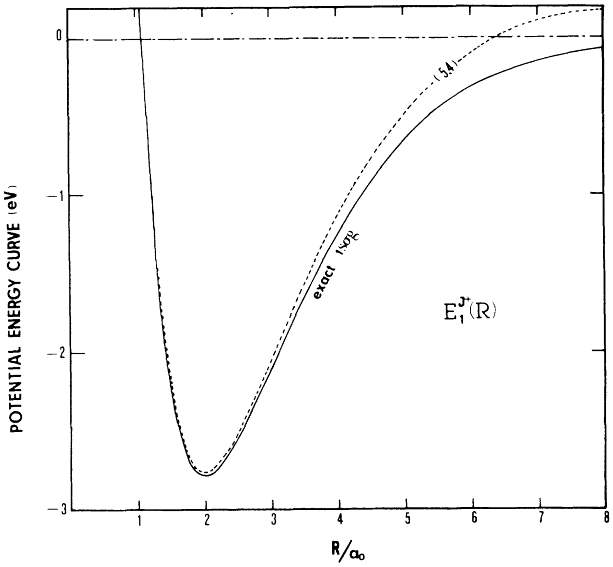

FIG. 5. Potential energy curve (eV) vs R (Bohr radii). The solid line denotes the exact $1s\sigma g$ potential (Ref. 7) while the dotted line is the result of our calculation for 15 terms in the expansion of v. $(n_{\max},l_{\max})=(5.4)$.

TABLE IV. Weight factors $\bar{G}_1^{0+}(R;ull)$ at $R=4a_0$ for increasing number of terms used in the separable representation of v.

State			$(n_{\max},l_{\max})$		
(nl)	(1,0)	(2,1)	(3,2)	(4,3)	(5,4)
$(1s)$	1.41	1.21	1.14	1.16	1.18
$(2s)$		-2.44×10^{-1}	-2.63×10^{-1}	-2.61×10^{-1}	-2.53×10^{-1}
$(3s)$			-1.19×10^{-1}	1.11×10^{-1}	1.01×10^{-1}
$(4s)$				-2.79×10^{-2}	-2.71×10^{-2}
$(5s)$					-5.27×10^{-3}
$(2p)$		-2.81×10^{-1}	-2.62×10^{-1}	-2.24×10^{-1}	-2.01×10^{-1}
$(3p)$			-1.73×10^{-1}	1.52×10^{-1}	1.41×10^{-1}
$(4p)$				-5.49×10^{-2}	-5.71×10^{-2}
$(5p)$					-3.22×10^{-3}
$(3d)$			-1.45×10^{-1}	-1.28×10^{-1}	-1.29×10^{-1}
$(4d)$				-8.25×10^{-2}	8.89×10^{-2}
$(5d)$					-1.12×10^{-2}
$(4f)$				9.10×10^{-2}	9.44×10^{-2}
$(5f)$					-3.81×10^{-2}
$(5g)$					6.30×10^{-2}

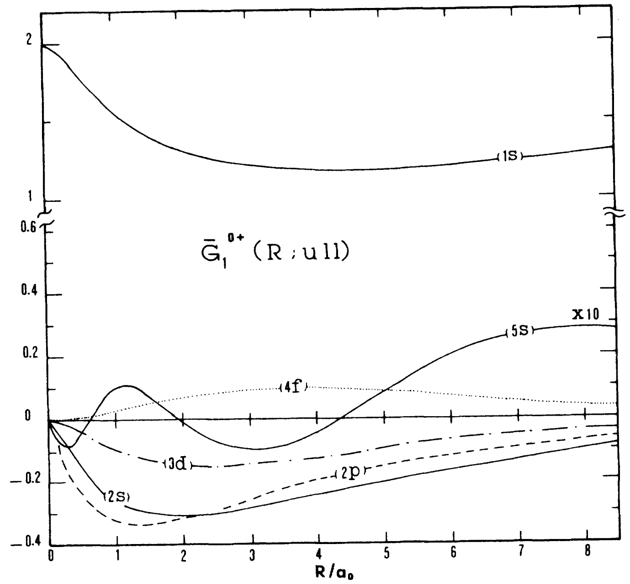

FIG. 6. Weight factors $\bar{C}_1^{0+}(R;ull)$ vs R (Bohr radii) for several hydrogenic states (nl) included in a 15-term expansion of v. $(n_{\max},l_{\max})=(5,4)$.

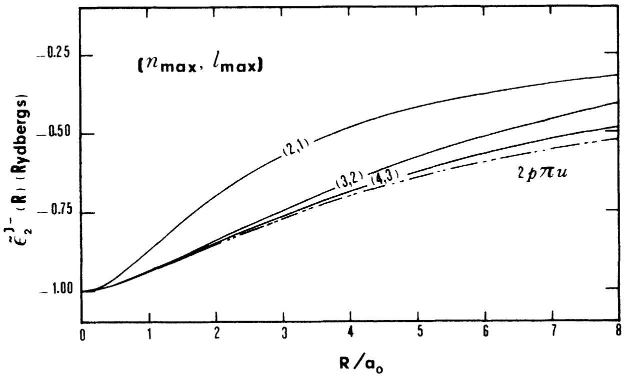

FIG. 8. Same as in Fig. 4 for $\tilde{\varepsilon}_1^{J-}(R)$. The dash–double-dotted line is the exact $2p\pi u$ result (Ref. 7).

Next we study the energy curves corresponding to $2p\sigma u$ and $2p\pi u$ which, respectively, bear support on the $(1s)$ and $(2p_x)$ hydrogen states of the separated-atom limit. These states start at -1 Ry from the united-atom $(2p)$ state and end up, respectively, -1 and $-\frac{1}{4}$ in the separated-atom limit. Therefore we need at least three terms in the expansion of v in order to include all hydrogenic states up to $n_{\max}=2$, $l_{\max}=1$. Since these are odd parity states we study $J^{(-)}$ configurations only. The lowest one corresponding to $2p\sigma u$ is denoted $\tilde{\varepsilon}_1^{J-}(R)$ while the second one corresponding to $2p\pi u$ is denoted $\tilde{\varepsilon}_2^{J-}(R)$. As mentioned before, $\tilde{\varepsilon}_i^{J-}(R)$ does not depend on J. In Figs. 7 and 8 we depict $\tilde{\varepsilon}_1^{J-}(R)$ and $\tilde{\varepsilon}_2^{J-}(R)$ for increasing $(n_{\max},l_{\max})$ states, and in Tables V and VI the calculated $\varepsilon_1^{J-}(R)$ and $\varepsilon_2^{J-}(R)$ are shown in increasing number of separable terms together with known exact results. Again we find that the calculated $\varepsilon_i^{J-}(R)$ appears to converge monotonically to the exact energy curves which clearly shows the validity of our method. Improved accuracy should result by increasing $n_{\max}$ and $l_{\max}$, which we could not do, due to computer limitations on the Vax 730 we used.

Finally, we look upon higher J^+ states involving the $2s\sigma g$ and $3d\sigma g$. Both bare support on the $(2s,2p_z)$ (Ref. 7) separated-atom states and intersect each other between $4a_0$ and $4.2a_0$. These energies are calculated in the rest frame of the molecule where $\mathbf{R}$ is fixed. In our work the electronic energies ε (or $\tilde{\varepsilon}$) are calculated in the frame where the molecule is rotating with total angular momentum J. As a result we find that curve crossing is inhibited. This is shown in Fig. 9 for $\tilde{\varepsilon}_i^{J+}(R)$ where $i=2$ corresponds to $2s\sigma g$ and $i=3$ to $3d\sigma g$. The calculated electronic energy $\varepsilon_2^{J+}(R)$ coincides with $2s\sigma g$ for $R<4a_0$ and becomes $3d\sigma g$ for $R>5a_0$. Likewise, $\varepsilon_3^{J+}(R)$ converges to $3d\sigma g$ for $R<4a_0$ but equals $2s\sigma g$

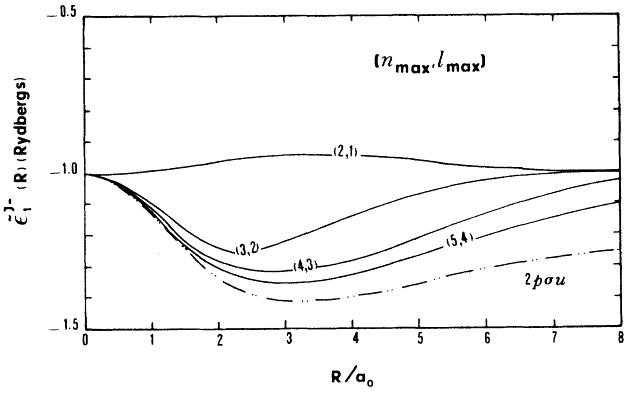

FIG. 7. Same as in Fig. 4 for $\tilde{\varepsilon}_1^{J-}(R)$. The dash–double-dotted line is the exact $2p\sigma u$ result (Ref. 7).

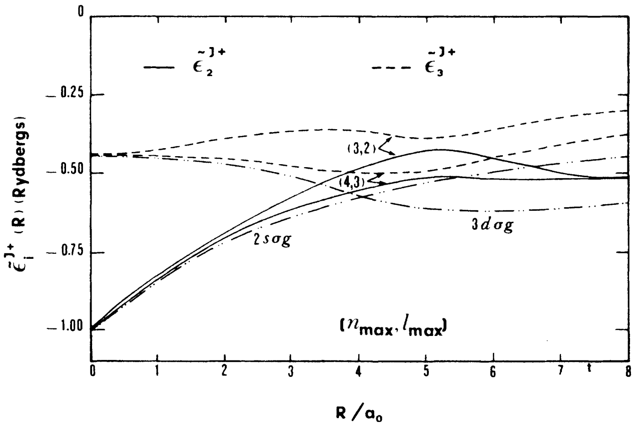

FIG. 9. Same as in Fig. 4 for $\tilde{\varepsilon}_2^{J+}(R)$ (solid lines) and $\tilde{\varepsilon}_3^{J+}(R)$ (dashed lines). The dash–double-dotted lines are the exact $2s\sigma g$ and $3d\sigma g$ results (Ref. 7).

TABLE V. Same as in Table III for $-\varepsilon_2^{J-}(R)$. The exact $2p\sigma u$ result is shown for comparison.

	$(n_{\max}, l_{\max})$				
R/a_0	(2,1)	(3,2)	(4,3)	(5,4)	$2p\sigma u$ exact
0.0	1.0000	1.000 00	1.000 00	1.000 00	1.000 00
0.2	1.005 32	1.005 32	1.005 34	1.005 35	1.005 35
0.4	1.021 04	1.021 26	1.021 45	1.021 50	1.021 58
0.6	1.046 32	1.047 19	1.048 08	1.048 33	1.048 61
0.8	1.079 41	1.081 36	1.083 95	1.084 73	1.085 48
1.0	1.117 80	1.120 93	1.126 47	1.128 16	1.129 62
1.2	1.158 57	1.162 67	1.172 17	1.174 97	1.177 22
1.4	1.198 86	1.203 73	1.217 38	1.221 19	1.224 15
1.6	1.236 37	1.241 91	1.285 99	1.263 55	1.267 21
1.8	1.269 56	1.275 72	1.294 94	1.300 04	1.304 46
2.0	1.297 66	1.304 28	1.324 28	1.329 88	1.335 07
2.2	1.320 48	1.327 36	1.346 95	1.353 14	1.359 12
2.4	1.338 27	1.345 21	1.363 48	1.370 40	1.377 15
2.6	1.351 52	1.358 43	1.374 67	1.382 39	1.389 91
2.8	1.360 84	1.367 71	1.381 45	1.389 90	1.398 22
3.0	1.366 84	1.373 74	1.384 63	1.393 69	1.402 85
3.2	1.370 11	1.377 12	1.384 95	1.394 46	1.404 43
3.4	1.371 17	1.378 36	1.382 97	1.392 85	1.403 58
3.6	1.370 47	1.377 85	1.379 16	1.389 38	1.400 82
3.8	1.368 36	1.375 92	1.373 94	1.384 48	1.396 54
4.0	1.365 15	1.372 81	1.367 64	1.378 49	1.391 10
5.0	1.339 36	1.345 77	1.329 78	1.339 64	1.354 58
6.0	1.307 02	1.301 19	1.295 66	1.296 73	1.314 62
7.0	1.274 75	1.275 49	1.268 59	1.258 83	1.278 26
8.0	1.245 59	1.245 44	1.243 94	1.230 72	1.247 21
9.0	1.220 51	1.220 27	1.220 38	1.211 29	1.221 31

TABLE VI. Same as in Table III for $-\varepsilon_2^{J-}(R)$. The exact $2p\pi u$ result is shown for comparison.

	$(n_{\max}, l_{\max})$				
R/a_0	(2,1)	(3,2)	(4,3)	(5,4)	$2p\pi u$ exact
0.0	1.000 00	1.000 00	1.000 00	1.000 00	1.000 00
0.2	0.997 38	0.997 37	0.997 38	0.997 38	0.997 40
0.4	0.989 90	0.989 83	0.989 91	0.989 93	0.989 93
0.6	0.978 41	0.978 17	0.978 49	0.978 57	0.978 60
0.8	0.963 88	0.963 41	0.964 16	0.964 32	0.964 39
1.0	0.947 15	0.946 52	0.947 81	0.948 09	0.948 21
1.2	0.928 96	0.928 32	0.930 22	0.930 60	0.930 78
1.4	0.909 89	0.909 42	0.911 88	0.912 41	0.912 65
1.6	0.890 40	0.890 24	0.893 25	0.893 92	0.894 22
1.8	0.870 82	0.871 08	0.874 61	0.875 43	0.875 79
2.0	0.851 40	0.852 11	0.856 17	0.857 14	0.857 55
2.2	0.832 32	0.833 46	0.838 07	0.839 18	0.839 65
2.4	0.813 71	0.815 23	0.820 40	0.821 65	0.822 18
2.6	0.795 65	0.797 48	0.803 21	0.804 61	0.805 21
2.8	0.778 18	0.780 25	0.786 55	0.788 08	0.788 78
3.0	0.761 33	0.763 56	0.770 41	0.772 08	0.772 89
3.2	0.745 12	0.747 45	0.754 81	0.756 63	0.757 56
3.4	0.729 55	0.731 91	0.739 73	0.741 72	0.742 78
3.6	0.714 60	0.716 96	0.725 16	0.727 34	0.728 54
3.8	0.700 26	0.702 57	0.711 10	0.713 48	0.714 84
4.0	0.686 52	0.688 75	0.697 52	0.700 12	0.701 65
5.0	0.625 92	0.627 56	0.636 24	0.640 34	0.642 77
6.0	0.576 82	0.577 73	0.584 44	0.590 50	0.593 98
7.0	0.536 75	0.536 94	0.540 37	0.548 38	0.553 26
8.0	0.503 78	0.503 35	0.502 78	0.512 23	0.519 02
9.0	0.476 45	0.475 61	0.470 74	0.480 80	0.490 05

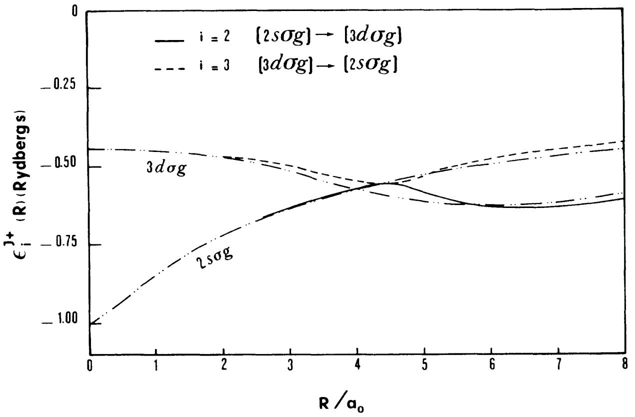

FIG. 10. Calculated electronic binding energy $\varepsilon_2^{J+}(R)$ (solid lines) an $\varepsilon_3^{J+}(R)$ (dashed lines) with $(n_{\max},l_{\max})=(4,3)$. The dash–double-dotted lines are in the exact $2s\sigma g$ and $3d\sigma g$ results (Ref. 7).

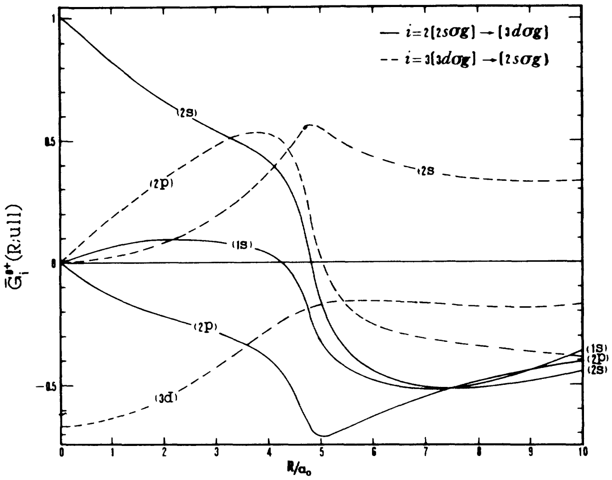

FIG. 11. Weight factors $\bar{G}_i^{0+}(R;ull)$ vs R (Bohr radii) for several hydrogenic states (nl) included in a ten-term expansion of v. $(n_{\max},l_{\max})=(4,3)$.

for $R>5a_0$. In Fig. 10 we depict the exact $2s\sigma g$ and $3d\sigma g$ curves as well as the calculated $\varepsilon_1^{J+}(R)$ and $\varepsilon_2^{J+}(R)$ for $(n_{\max},l_{\max})=(4,3)$. In Table VII we display the corresponding numerical values to show the accuracy of the calculation and in Fig. 11, for $(n_{\max},l_{\max})=(4,3)$, we show the $\bar{G}_i^{J+}(R,c)$ as a function of R for the asymptotic channels c that correspond to $(2s)$ and $(2p)$ states. We find that around $R=4.8a_0$ the $\bar{G}$'s change rapidly with R and for $R>10a_0$ the weight factors for the $(2s)$ and $(2p)$ states are the only ones to remain finite. Comparing the $(2s)$ and $(2p)$ weight factors corresponding to different molecular-orbital states $i=2$ and 3 we find that there is no indication of curves crossing in the solution of the equations we propose here. Instead, the curves smoothly tough each other. As discussed below this result may shed light on the complicated problem of inhibited curve crossing in molecular physics. The noncrossing rule that was first pointed out by Neumann and Wigner[23] states that "for an infinitely slow change of internuclear distance two electronic states of the same species (same symmetry properties) cannot cross each other." It does happen frequently that in a certain approximation two potential curves of the same species intersect; but according to the noncrossing rule in a sufficiently high approximation this interaction is avoided, that is, the upper curve on the

TABLE VII. Same as in Table III for $-\varepsilon_2^{J+}(R)$ and $-\varepsilon_3^{J+}(R)$. The exact $2s\sigma u$ and $3d\sigma g$ results are shown for comparison.

			$-\varepsilon_2^{J+}(R)$			$-\varepsilon_3^{J+}(R)$		
R/a_0	$2s\sigma g$ exact	(5,4)	(4,3)	(3,2)	(3,2)	(4,3)	(5,4)	$3d\sigma g$ exact
0.0	1.000 00	1.000 00	1.000 00	1.000 00	0.444 44	0.444 44	0.444 44	0.444 44
1.0	0.845 85	0.844 88	0.843 76	0.838 39	0.449 77	0.449 84	0.450 23	0.450 37
2.0	0.721 73	0.719 99	0.717 53	0.712 37	0.464 41	0.466 07	0.469 80	0.471 55
3.0	0.637 77	0.634 72	0.631 45	0.625 50	0.492 81	0.497 51	0.508 38	0.515 00
3.2	0.624 12	0.620 70	0.617 42	0.611 57	0.501 34	0.505 92	0.518 27	0.526 12
3.4	0.611 29	0.607 51	0.604 22	0.598 60	0.511 13	0.514 96	0.528 54	0.537 61
3.6	0.599 21	0.595 09	0.591 80	0.586 54	0.522 20	0.524 48	0.538 93	0.549 19
3.8	0.587 80	0.583 49	0.580 19	0.575 36	0.534 46	0.534 27	0.549 09	0.560 56
4.0	0.577 03	0.573 03	0.569 50	0.565 06	0.547 66	0.543 97	0.558 40	0.571 45
4.2	0.566 84	0.565 61	0.560 16	0.555 75	0.561 28	0.552 84	0.564 75	0.581 61
4.4	0.557 17	0.568 08	0.553 45	0.547 69	0.574 56	0.559 24	0.561 22	0.590 86
4.6	0.548 01	0.578 70	0.553 19	0.541 61	0.586 37	0.559 20	0.548 96	0.599 05
4.8	0.539 29	0.587 68	0.565 15	0.539 43	0.594 61	0.547 68	0.537 81	0.606 11
5.0	0.531 01	0.594 60	0.583 58	0.546 04	0.593 90	0.530 46	0.528 25	0.612 02
6.0	0.495 11	0.612 23	0.625 23	0.632 45	0.491 55	0.479 19	0.489 90	0.624 99
7.0	0.466 56	0.609 95	0.626 98	0.637 13	0.459 90	0.445 90	0.459 21	0.616 84
8.0	0.443 55	0.595 15	0.609 33	0.610 14	0.438 88	0.420 00	0.433 11	0.597 02
9.0	0.424 83	0.573 70	0.582 14	0.574 83	0.422 50	0.400 15	0.410 56	0.572 22

right of the point of intersection goes over into the upper curve on the left and the lower curve on the right goes to the lower curve on the left. In the H_2^+ molecule the lower approximation involves the solution of the two-center problem in the rest frame of the molecule where $\mathbf{R}$ is fixed. As calculated in Ref. 7 this leads to curve crossing for the $2s\sigma d$ and $3d\sigma d$ energy states. In our work the distance R is fixed but $\mathbf{R}$ can rotate with angular momentum L such that $L+l$ couple to total angular momentum J (l is angular momentum of the electron). Therefore we conclude that in H_2^+ noncrossing of electronic states of the same species is due to the correct treatment of angular-momentum states so that the two-center eigenfunction may have well-defined J and P.

After we have shown how the results of our work reproduce with reasonable accuracy the known exact electronic binding energies for different molecular orbitals of the H_2^+ molecule, the only thing left is to solve the set of coupled differential equations (78) to obtain, for each J and P, the energy levels of the H_2^+ molecule. For the low-lying states one may proceed as in the Born-Oppenheimer approximation to neglect the coupling to other molecular-orbital states other than the $1s\sigma g$. For $(n_{\max}, l_{\max})=(5,4)$ this amounts to the solution of 15 coupled equations for $J^P=0^+$, 31 for 2^+, and 35 for $J\geq 4$. Using the spline method[24] we are in the process of developing a bound-state code[25] for the solution of a general coupled-channel problem that allows for large number of channels and provides at least four-digit accuracy. For this reason the results of such work will be reported at a later time.

VI. CONCLUSION

In the present work we have developed a nonvariational parameter-free approach to the molecular three-body problem which is based on the exact solution of the Faddeev two-center Hamiltonian h given in (5) for a separable representation of the light-heavy potential v through the Hilbert-Schmidt method. The wave function Ψ of the full three-body Hamiltonian H with total angular momentum J and parity P is written in the form of an ansatz involving the channel components $\bar{\psi}^{ic}$ of the Faddeev two-center eigenfunctions we solved first with a separable v and unknown coefficients Φ^{ic} that depend only on the distance R between the two heavy particles. Based on the above-mentioned ansatz for Ψ, we were able to formulate a set of coupled differential equations for the unknowns Φ^{ic} which are formally exact equations for the molecular three-body problem. Therefore the wave function Ψ we get has well-defined angular momentum J and parity P and is a nonvariational parameter-free rotationally invariant solution of H.

As a first attempt to test this new molecular approach proposed here, we have solved the resulting equations for the H_2^+ molecule. For each J and P, we have calculated the electronic binding energy for different molecular-orbital states as a function of R. We find that for increasing number of terms in the separable representation of v the results of our calculation appear to converge monotonically to exact electronic energies corresponding to $1s\sigma g$, $2p\sigma u$, $2p\pi u$, $2s\sigma g$, and $3d\sigma g$. Reasonable accuracy is reached for 15 terms in the expansion of v which amounts to including all hydrogenic states up to $(5g)$. Computer limitations prevented us from going any further at this time. Although we are using a global basis set to span v, we find no difficulty in getting monotonic convergence for all molecular-orbital states we have tried, including $2s\sigma g$ and $3d\sigma g$ which asymptotically couple to different hydrogenic states. This may be due to the nonvariational nature of our calculation where the two-center eigenfunctions ψ_i^{JP} are obtained from the exact solution of an homogeneous equation whose solution only exists for discrete $\bar{\varepsilon}_i^{JP}(R)$. As more terms in the separable expansion of v are included the $\bar{\varepsilon}_i^{JP}(R)$ approach the corresponding exact molecular energy curves, and the weight factors $\bar{G}_i^{JP}(R;c)$ with which each hydrogenic state (nl) contributes to ψ_i^{JP} in channel c are exactly adjusted through the solution of an eigenvalue problem. This natural adjustment may be the key to the observed monotonic convergence for $\varepsilon_i^{JP}(R)$ once the dominant hydrogenic states at a given R are included. Therefore we expect to be able to reach four- or five-digit accuracy in the range $0<R<10a_0$ once the computer facilities at our disposal allow us to go above $(n_{\max}, l_{\max})=(5,4)$.

Another great advantage in our method is the use of the Hilbert-Schmidt expansion for the electron-proton Coulomb potential. This method is the only one that provides an exact solution of the two-center problem at both $R=0$ and $R=\infty$ for all molecular-orbital states one might consider. Therefore having naturally constrained an exact result at both extremes the convergence in between follows from the correct treatment of the dynamics in the frame where the molecule rotates. Finally, in the framework of our method electronic energy curves that cross each other in the rest frame of the molecule ($\mathbf{R}$ fixed) smoothly touch each other in the frame where the molecule rotates with total angular momentum J and parity P. This confirms the noncrossing rule of Neumann and Wigner[23] and shows how with few terms in the expansion of v and the correct treatment of the dynamics we get the needed electronic molecular energy curves and simultaneously provide a simple interpretation for the noncrossing rule in H_2^+

Although further work is still needed to solve the coupled set of differential equations in each J^P we expect our method to provide very accurate results for the energy levels of the H_2^+ molecule as well as wave functions with good J and P that may be used to calculate transition rates involving rotational and vibrational levels. Furthermore, we expect to be able to generalize the method so that it may be used in more complicated diatomic or triatomic molecules such as H_2, H_3^{+2}, and others, not to mention its application to the understanding of the $dd\mu$ mesonic molecule. Since $m_\mu/m_e \simeq 250$ we expect factors of $\mathcal{m}/\mathcal{M}$ to contribute more than in H_2^+. Nevertheless, due to the nature of our formulation we expect to be able to account for some of these factors. Work in some of these problems is currently underway.

APPENDIX A: WEINBERG NATURAL EXPANSION

Let v be a two-body potential and $g_0(\mathcal{E})$ the free resolvent whose momentum-space representation is given by

$$\langle \mathbf{k}' \,|\, g_0(\mathcal{E}) \,|\, \mathbf{k} \rangle = \left[\mathcal{E} - \frac{\hbar^2}{2\nu} k^2 \right]^{-1} \delta(\mathbf{k}-\mathbf{k}') \,, \tag{A1}$$

where $\mathcal{E}$ is the two-body center-of-mass energy and ν the appropriate reduced mass. In momentum space the Lippmann-Schwinger equation for the t matrix reads

$$\langle \mathbf{k}' \,|\, t(\mathcal{E}) \,|\, \mathbf{k} \rangle = \langle \mathbf{k}' \,|\, v \,|\, \mathbf{k} \rangle + \int \frac{d^3k''}{(2\pi)^3} \langle \mathbf{k}' \,|\, v \,|\, \mathbf{k}'' \rangle \left[\mathcal{E} - \frac{\hbar^2}{2\nu} k''^2 \right]^{-1} \langle \mathbf{k}'' \,|\, t(\mathcal{E}) \,|\, \mathbf{k} \rangle \,, \tag{A2}$$

which after partial wave decomposition becomes

$$t_l(\mathcal{E};k',k) = v_l(k'k) + \int_0^\infty \frac{k''^2 dk''}{2\pi^2} v_l(k',k'') \times \left[\mathcal{E} - \frac{\hbar^2}{2\nu} k''^2 \right]^{-1} t_l(\mathcal{E};k'',k) \,, \tag{A3}$$

where

$$\langle \mathbf{k}' \,|\, v \,|\, \mathbf{k} \rangle = \sum_{l,m} 4\pi v_l(k',k) Y_{lm}^*(\hat{\mathbf{k}}') Y_{lm}(\hat{\mathbf{k}}) \,. \tag{A4}$$

In operator form we may write (A3) as

$$t_l(\mathcal{E}) = v_l + v_l g_0(\mathcal{E}) t_l(\mathcal{E}) \,, \tag{A5}$$

whose Kernel is $v_l g_0(\mathcal{E})$. In the Weinberg[15] natural expansion one uses the eigenvectors of the kernel to represent v in a separable form. From

$$v_l g_0(\mathcal{E}) \,|\, \xi_u^l(\mathcal{E}) \rangle = \eta_u^l(\mathcal{E}) \,|\, \xi_u^l(\mathcal{E}) \rangle \,, \tag{A6}$$

and

$$g_0(\mathcal{E}) v_l \,|\, \psi_u^l(\mathcal{E}) \rangle = \eta_u^l(\mathcal{E}) \,|\, \psi_u^l(\mathcal{E}) \rangle \,, \tag{A7}$$

one obtains the right and left eigenfunctions of $v_l g_0(\mathcal{E})$ for the same eigenvalue $\eta_u^l(\mathcal{E})$. The index u denotes the different eigenvalues of v_l at $\mathcal{E}$. The eigenfunctions of ξ_u^l are usually normalized such that

$$\langle \xi_{u'}^l(\mathcal{E}) \,|\, g_0(\mathcal{E}) \,|\, \xi_u^l(\mathcal{E}) \rangle = -\delta_{uu'} \,. \tag{A8}$$

Using the eigenfunctions ξ_u^l it can be shown[15] that v_l may be written as

$$v_l = \sum_u^{N_l} |\, \xi_u^l(\mathcal{E}) \rangle \eta_u^l(\mathcal{E}) \langle \xi_u^l(\mathcal{E}) \,| \,, \tag{A9}$$

which once substituted in (A5) leads, with the help of (A8), to

$$t_l = \sum_u^{N_l} |\, \xi_u^l(\mathcal{E}) \rangle \tau_u^l(\mathcal{E}) \langle \xi_u^l(\mathcal{E}) \,| \,, \tag{A10}$$

$$\tau_u^l(\mathcal{E}) = \frac{-\eta_u^l(\mathcal{E})}{1-\eta_u^l(\mathcal{E})} \,, \tag{A11}$$

where N_l is the number of eigenfunctions used to represent v. Comparing (A6) with (A7) one may easily relate ξ with ψ,

$$|\, \psi_u^l(\mathcal{E}) \rangle = g_0(\mathcal{E}) \,|\, \xi_u^l(\mathcal{E}) \rangle \,. \tag{A12}$$

The full momentum-space representation of the t matrix reads

$$\langle \mathbf{k}' \,|\, t(\mathcal{E}) \,|\, \mathbf{k} \rangle = \sum_u^{N_l} \sum_{l,m} 4\pi Y_{lm}^*(\hat{\mathbf{k}}') \xi_u^l(\mathcal{E};k') \tau_u^l(\mathcal{E}) \times \xi_u^l(\mathcal{E};k) Y_{lm}(\hat{\mathbf{k}}) \,. \tag{A13}$$

If the potential v has a bound state at $\mathcal{E} = \varepsilon_0$ in $l = 0$ then $\eta_1^0(\varepsilon_0) = 1$. If a second one exists at $\mathcal{E} = \varepsilon_1$ then $\eta_2^0(\varepsilon_1) = 1$ while $\eta_1^0(\varepsilon_1) > 1$. The same happens for $l > 0$. Therefore t_l develops a pole at the bound-state energies through $\eta_u^l(\mathcal{E})$. For potentials $v(r)$ that are attractive for all r the η's are positive for $-\infty < \mathcal{E} < 0$ and $\eta_u^l(-\infty) = 0$. The index u denotes the number of nodes of the eigenfunction ξ_u^l. The eigenfunctions corresponding to the lowest eigenvalue ($u = 1$) has zero nodes; the number of nodes increases with u.

APPENDIX B: BOUND-STATE FORM FACTORS OF THE HYDROGEN ATOM

The radial part of the hydrogen wave function is given by the well-known expression[26]

$$R_{nl}(r) = (n\alpha_n)^{3/2} \frac{2}{n^2} \left[\frac{(n-l-1)!}{(n+l)!^3} \right]^{1/2} (2\alpha_n r)^l e^{-\alpha_n r} \times L_{n-l-1}^{2l+1}(2\alpha_n r) \,, \tag{B1}$$

where n is the principal quantum number, l the orbital angular momentum, and L the Laguerre polynomial. The corresponding binding energy is ε_n and $\alpha_n = \sqrt{-2\nu/\hbar^2 \varepsilon_n}$ where ν is given by (11). Using a power-series representation for L,

$$L_{n-l-1}^{2l+1}(x) = \sum_{s=0}^{n-l-1} (-1)^s \frac{(n+l)!^2}{(n-l-1-s)!(2l+1+s)!s!} x^s \,, \tag{B2}$$

we get

$$R_{nl}(r)=2\alpha_n^{3/2}\left[\frac{(n-l-1)!(n+l)!}{n}\right]^{1/2}(2\alpha_n r)^l e^{-\alpha_n r}$$

$$\times\sum_{s=0}^{n-l-1}\frac{(-1)^s(2\alpha_n r)^s}{(n-l-1-s)!(2l+1+s)!s!}\ . \tag{B3}$$

The total wave function $\mathcal{U}$ for the state with quantum numbers nlm is

$$\mathcal{U}_{nlm}(\mathbf{r})=R_{nl}(r)Y_{lm}(\hat{\mathbf{r}})\ , \tag{B4}$$

whose Fourier transforms is

$$\mathcal{U}_{nlm}(\mathbf{k})=R_{nl}(k)Y_{lm}(\hat{\mathbf{k}}) \tag{B5}$$

where

$$R_{nl}(k)=(-i)^l 4\pi\int_0^\infty r^3 dr\, R_{nl}(r)j_l(kr)\ . \tag{B6}$$

Using the relation

$$j_l(x)=\left[\frac{\pi}{2x}\right]^{1/2}J_{l+1/2}(x)\ , \tag{B7}$$

where J is a Bessel function of fractional order, together with

$$\int_0^\infty dr\, r^{l+1/2+1+s}e^{-\alpha r}J_{l+1/2}(kr)$$

$$=(-1)^s\left[\frac{d}{d\alpha}\right]^s 2\alpha\left[\frac{2k}{\pi}\right]^{1/2}\frac{2^l(l+1)!k^l}{(\alpha^2+k^2)^{l+2}}\ , \tag{B8}$$

we get

$$R_{nl}(k)=(-i)^l 4\pi 2\alpha_n^{3/2}(4\alpha_n k)^l\left[\frac{(n-l-1)!(n+l)!}{n}\right]^{1/2}(l+1)!$$

$$\times\sum_{s=0}^{n-l-1}\frac{(2\alpha_n)^s}{(n-l-1-s)!(2l+1+s)!s!}\left[\frac{d}{d\alpha_n}\right]^s\left[\frac{2\alpha_n}{(\alpha_n^2+k^2)^{l+2}}\right]\ . \tag{B9}$$

The corresponding hydrogen-atom bound-state form factor is obtained from

$$|f_{nlm}\rangle=v\,|\mathcal{U}_{nlm}\rangle=g_0^{-1}(\varepsilon_n)\,|\mathcal{U}_{nlm}\rangle\ , \tag{B10}$$

where $v=Ze^2/r$. In units of $\hbar=2\nu=1$ we write $f_{nlm}(\mathbf{k})$ as

$$f_{nlm}(\mathbf{k})=-(\alpha_n^2+k^2)i^l\mathcal{U}_{nlm}(\mathbf{k})=\sqrt{4\pi}f_{nl}(k)Y_{lm}(\hat{\mathbf{k}})\ , \tag{B11}$$

where the i^l factor is added to make $f_{nl}(k)$ a real function of k. Comparing (B11) with (B5) we get

$$f_{nl}(k)=-\frac{\alpha_n^2+k^2}{\sqrt{4\pi}}i^l R_{nl}(k)\ , \tag{B12}$$

where $R_{nl}(k)$ is given by (B9). If in addition to $\hbar=2\nu=1$ the rydberg is taken as the unit of energy we have

$$\varepsilon_n=-Z^2/n^2\ , \tag{B13}$$

$$\alpha_n=\sqrt{-\varepsilon_n}=Z/n\ , \tag{B14}$$

$$v(r)=-2Z/r\ , \tag{B15}$$

where r is in units of Bohr radius. The charge number Z of the atomic nucleus which is $Z=1$ for hydrogen is left here unspecified for generality of presentation.

APPENDIX C: EIGENFUNCTION OF THE COULOMB KERNEL

Since the Coulomb potential $v(r)$ given in (B15) is responsible for an infinity of bound states at $\varepsilon_n=-Z^2/n^2$, one can easily determine the eigenvalues η and eigenfunction ξ of the Coulomb Kernel $vg_0(\mathcal{E})$ at any negative energy $\mathcal{E}$. Going back to (A7) we note that it may be rewritten as

$$\frac{1}{\eta(\mathcal{E})}v\,|\psi(\mathcal{E})\rangle=g_0^{-1}(\mathcal{E})\,|\psi(\mathcal{E})\rangle\ , \tag{C1}$$

which in coordinate space is nothing but the Schrödinger equation for the wave function ψ. The corresponding binding energy is $\mathcal{E}$ and the effective potential is

$$v'=v/\eta(\mathcal{E})=-2Z'/r\ , \tag{C2}$$

where

$$Z'=Z/\eta(\mathcal{E})\ . \tag{C3}$$

Therefore $\mathcal{E}$ must satisfy the relation

$$\mathcal{E}=-(Z'/n)^2=-Z^2/[n\eta(\mathcal{E})]^2\ , \tag{C4}$$

which leads to

$$\frac{1}{\eta(\mathcal{E})}=\frac{n}{Z}\sqrt{-\mathcal{E}}=\frac{n}{Z}\delta\ . \tag{C5}$$

Therefore we may denote the eigenvalues of vg_0 as $\eta_n(\mathcal{E})$ and the corresponding eigenfunctions as $\xi_n^l(\mathcal{E})$ and $\psi_n^l(\mathcal{E})$. As mentioned in Appendix A the η_n become unity when $\mathcal{E}=-Z^2/n^2$. Because of (A12) and (A18) the ξ are related to the f's defined in Appendix B. If in (B9) and (B12) we change α_n into $\delta=\sqrt{-\mathcal{E}}$ we may write

$$\xi_n^l(\mathcal{E};k)=\frac{1}{\sqrt{2\delta}}[f_{nl}(k)]_{\alpha_n=\sqrt{-\mathcal{E}}}\ , \tag{C6}$$

where the $\sqrt{2}\delta$ factor is responsible for the normalization condition (A8).

Since the quantum numbers n and l satisfy the condition $n \geq l+1$ we rather index η and ξ through u and l. For a given l, u runs from one to a maximum value N_l. Given u and l we denote the eigenvalues and eigenvectors as η_u^l and ξ_u^l where

$$n = u + l \ . \tag{C7}$$

Therefore, defining $\delta = \sqrt{-\mathcal{E}}$, we get

$$\xi_1^0(\mathcal{E};k) = -\frac{\sqrt{4\pi}}{\sqrt{2\delta}} \frac{4\delta^{5/2}}{k^2+\delta^2} \ , \tag{C8}$$

$$\xi_2^0(\mathcal{E};k) = -\frac{\sqrt{4\pi}}{\sqrt{2\delta}} \frac{8\delta^{5/2}}{(k^2+\delta^2)^2}(k^2-\delta^2) \ , \tag{C9}$$

$$\xi_1^1(\mathcal{E},k) = -\frac{\sqrt{4\pi}}{\sqrt{2\delta}} \frac{16}{3}\delta^{7/2} \frac{k}{(k^2+\delta^2)^2} \ , \tag{C10}$$

for the first three eigenfunctions.

---

[1] L. D. Faddeev, Zh. Eksp. Teor. Fiz. **39**, 1459 (1960) [Sov. Phys.—JETP **12**, 1014 (1961)].

[2] F. S. Levin, in *Proceedings of the Ninth International Conference on the Few-Body Problem,* edited by F. S. Levin (North-Holland, Amsterdam, 1981).

[3] H. van Haeringen, *Charged-Particle Interactions* (Coulomb, Leiden, 1985).

[4] T. K. Lim, in *Few-Body Problems in Physics,* edited by B. Zeitnitz (North-Holland, Amsterdam, 1984).

[5] M. Born and R. Oppenheimer, Ann. Phys. **84**, 457 (1927).

[6] S. Gasiorowicz, *Quantum Physics* (Wiley, New York, 1974); F. Pilar, *Elementary Quantum Chemistry* (McGraw-Hill, New York, 1968).

[7] D. R. Bates, K. Ledsham, and A. L. Stewart, Philos. Trans. R. Soc. London, Ser. A **246**, 215 (1953); H. Wind, J. Chem. Phys. **42**, 2371 (1965).

[8] M. Kotani, K. Ohno, and K. Kayame, in *Molecules II,* Vol. 37 of *Encyclopedia of Physics,* edited by S. Flügge (Springer-Verlag, Berlin, 1961); G. Herzberg, *Molecular Spectra and Molecular Structure* (Van Nostrand Reinhold, New York, 1950).

[9] F. S. Levin and H. Krüger, Phys. Rev. A **15**, 2147 (1977).

[10] F. S. Levin, Phys. Rev. C **21**, 2199 (1980) and references therein.

[11] W. K. Ford and F. S. Levin, Phys. Rev. A **29**, 30 (1984).

[12] W. K. Ford and F. S. Levin, Phys. Rev. A **29**, 43 (1984).

[13] P. M. Prenter, *Splines and Variational Methods* (Wiley, New York, 1975).

[14] S. Weinberg, Phys. Rev. **131**, 440 (1963).

[15] S. Weinberg, Phys. Rev. **133**, B232 (1964).

[16] F. A. Gareev, M. Ch. Gizzatzulov, and J. Revai, Nucl. Phys. **A286**, 512 (1977).

[17] W. Glöckle, *The Quantum Mechanical Few-Body Problem* (Springer-Verlag, Heidelberg, 1983); *Models and Methods in Few-Body Physics,* Vol. 273 of *Lecture Notes in Physics,* edited by L. S. Ferreira, A. C. Fonseca, and L. Streit (Springer-Verlag, Heidelberg, 1987).

[18] E. W. Schmidt and H. Ziegelmann, *The Quantum Mechanical Three-Body Problem* (Pergamon, Oxford, 1974).

[19] M. L. Goldberger and K. M. Watson, *Collision Theory* (Wiley, New York, 1964).

[20] D. J. Ernest, C. M. Shakin, and R. M. Thaler, Phys. Rev. C **8**, 46 (1973).

[21] C. Lovelace, Phys. Rev. **135B**, 1225 (1964); M. G. Fuda, Nucl. Phys. **A116**, 83 (1968).

[22] S. K. Adhikari and I. H. Sloan, Phys. Rev. C **11**, 1133 (1975); Nucl. Phys. **A241**, 429 (1975).

[23] J. V. Neumann and E. Wigner, Phys. Z. **30**, 467 (1929).

[24] G. L. Payne, *Models and Methods in Few-Body Physics,* Vol. 273 of *Lecture Notes in Physics,* edited by L. S. Ferreira, A. C. Fonseca, and L. Streit (Springer-Verlag, Heidelberg, 1987).

[25] M. T. Pẽna and A. C. Fonseca (unpublished).

[26] A. Messiah, *Mècanique Quantique* (Dunod, Paris, 1965).